DESIGN OF THE ADVANCED REGIONAL AIRCRAFT, THE DART-75

A design project by students in the Department of Aerospace Engineering at Auburn University, Auburn, Alabama, under the sponsorship of NASA/USRA Advanced Design Program.

Auburn University
Auburn, Alabama
June 1992

AEROSPACE ENGINEERING AE 449

Auburn University

Auburn, Alabama

Design of the Advanced Regional Aircraft, the DART-75

Submitted to: Dr. James O. Nichols

Submitted by: Group II

Steve Elliott
Jason Gislason
Mark Huffstetler
Jon Mann
Ashley Withers
Mark Zimmerman

Date submitted: May 14, 1992

ABSTRACT

This design analysis is intended to show the capabilities of the DART-75, a 75 passenger medium-range regional transport. Included are the detailed descriptions of the structures, performance, stability and control, weight and balance, and engine design. The design should allow for the DART to become the premier regional aircraft of the future due to some advanced features like the canard, semi-composite construction, and advanced engines.

TABLE OF CONTENTS

LIST OF FIGURES

LIST OF FIGURES (continued)

LIST OF TABLES

LIST OF SYMBOLS

Symbol	Description	Units
A	Constant	
a_c	Lift Curve Slope of Canard	1/deg
a_t	Lift Curve Slope of Tail	1/deg
a_{wb}	Lift Curve Slope of Wing and Body	1/deg
B	Constant	
b	Span	ft
BPR	By Pass Ratio	
C	Constant	
c	Chord Length	ft
C_D	Drag Coefficient	
C_{Do}	Parasite Drag Coefficient	
C_f	Skin Friction Coefficient	
c.g.	Center of Gravity	
C_L	Coefficient of Lift	
$C_{m_{\alpha}cg}$	Moment About the Center of Gravity Slope Curve	1/deg
$C_{m_{\alpha}}$	Moment Slope Curve	1/rad
$C_{N_{\alpha}c}$	Normal Force Curve Slope for the Canard	1/deg
$C_{N_{\alpha}t}$	Normal Force Curve Slope for the Tail	1/deg
$C_{N_{\alpha}w}$	Normal Force Curve Slope for the Wing	1/deg
D	Constant	
d	Drag	lb
F	Force	lb

LIST OF SYMBOLS (continued)

F_g	Fuel Capacity	gal
h_n	Static Margin	
h_m	Maneuver Point	
h_{nwb}	Neutral Point of Wing Body	
K	Constant	
l_f	Length of Fuselage	ft
l_t	Moment Arm from Wing to Tail	ft
M	Mach Number	
mac	Mean Aerodynamic Chord	
N	Ultimate Load Factor	
$N_{subscript}$	Number of Components	
R	Range	nm
Re	Reynolds Number	
$S_{subscript}$	Area of Component	ft^2
t_r	Thickness of Root Chord	ft
TSFC	Thrust Specific Fuel Consumption	lb/hr/lb
V	Velocity	knots
V_c	Canard Volume	
V_D	Design Dive Speed	knots
V_H	Horizontal Tail Volume	
V_{pr}	Volume of Pressurized Space	ft^3
$W_{subscript}$	Weight of Component	lb
WZF	Zero Fuel Weight	lb

LIST OF SYMBOLS (continued)

x	Location of Center of Gravity	ft
x_{cp}	Location of Center of Pressure	ft
x_i	Component Center of Gravity Location	ft
z	Vertical Center of Gravity Location	ft
μ	Viscosity	slug/ft-s
ρ	Density	$slug/ft^3$
ρ_{sl}	Density at Sea Level	$slug/ft^3$

INTRODUCTION

In today's aviation industry the regional aircraft is a dying breed. This decline in regional aircraft can be traced to many causes. Perhaps the most significant cause is that these aircraft are inefficient. The average regional transport, such as the Fokker F28 and the Yakovlev Yak-40, have conventional designs from the early sixties. Designs like the Saab-Fairchild SF-340 have much more modern designs, but are aimed at the commuter market. Major aerospace companies such as McDonnell Douglas, British Aerospace, and others are directing development of new planes toward the above eighty passenger market. At this time, there is no American aerospace company that produces a regional transport for under 100 passengers.

The intention of the DART-75 is to fill this void with a modern, efficient regional aircraft. Therefore, it is of supreme importance that the DART be as efficient as possible. This efficiency can be achieved many ways, including: efficient aerodynamics, efficient engines, and a lightweight structure. However, efficiency is not the only consideration. Structural integrity, fatigue life, ease of maintenance, passenger comfort and convenience, and noise level must all be considered, along with many other considerations. These factors force the design team to face many tradeoffs that must be studied for the best solution. The final consideration that cannot be overlooked, is that of cost. The cost of the aircraft must remain competitive.

GENERAL DESIGN

The unique design configuration for the DART provides for a more efficient airplane. The configuration has three lifting surfaces, thus no aerodynamic lift downward is ever needed to trim the aircraft. Three lifting surfaces also provide more efficient take off and landing. Although the design increases drag through more surface area, it makes up for this effect through the increased overall design efficiency from the three lifting surfaces.

The basic configuration consists of a canard placed forward and low on the fuselage to decrease interference with the engine inlets at angles of attack. The wing is placed higher than the canard, at mid length of the body. Behind and slightly above the wing is the engine. This stacking effect will help eliminate the possibility of canard vortices entering the engine.

The semi-diamond shaped wings are not only aesthetically pleasing but are designed to provide efficient fuel placement. The large inner portion of the wing, where structural integrity is most easily maintained, is used to hold most of the fuel. The outer portion of the wing is left to hold mostly aerodynamic forces. Therefore the outer portion can be made lighter, thus decreasing overall weight of the aircraft. The inner portion of the diamond also provides for around half of the lift of the airplane, therefore maximizing efficiency though being structurally sound.

The choice of the wing airfoil proved to be a difficult task

since the wing shape was so unique. To eliminate the cost involved in the development of a new airfoil design, the NACA 2412 standard airfoil was adopted for the DART 75. This airfoil provides the lift and drag characteristics necessary for this design. By choosing an existing airfoil, more time was given to determine the actual flight characteristics of the uniquely designed wing.

The use of the tail, while providing only a marginal lift increase, is mainly used as a control surface and as a stability measure. The unique design is not only efficient but also aesthetically pleasing. The DART is 95 feet in length with a wing span of 75 feet. The semi-diamond shaped wing has an aspect ratio of 9.14. The canards and the tail both span 26 feet. The diameter of the body is 11 feet. The outer main dimensions can be seen in Figure 1.

The basic interior design of the DART is shown in Figure 2. The basic interior configuration consist of the two-place flight deck followed by the stewards area providing a galley with complimentary snacks and drinks, luggage bin and closet, as well as a lavatory. Across from the stewardess seat will be the main exit. This exit will be a door sliding up into the plane with stairs sliding into the fuselage under the doorway.

Following the stewards' area is the passenger compartment. The passengers will all ride coach sitting five abreast. The emergency exits will be stationed over the wings for the safety of the passengers. The rear stewards' section will consist of a

wardrobe closet, and an additional lavatory for the passengers' convenience.

A cross section of the aircraft interior cabin is provided in Figure 3. The middle seat of the three is provided with additional room for passenger comfort. The floor that is shown will also add structural integrity to the wings, The main support for the wings will be incorporated within the floor base. The overhead storage compartments will be large enough to hold a standard sized overnight bag along with a pillow and small blanket for each passenger. Traditional emergency lighting will also be included within the interior cabin.

Also considered very important for quick turnaround is the Ground Handling. Figure 4 is provided to show how ground crews will service the airplane. Even with the canard structure ground crews will have little difficulty serving the aircraft.

The characteristic loading of the DART is shown in Figure 5. The interior cabin is viewed to show the baggage compartment underneath the cabin. Also shown is the rear section with the luggage door placement. Information and help in obtaining a realistic general design was provided by Chief Engineer Mr. Mike Pulaski of USAir. The best existing technology from several aircraft are to the incorporated with the instrumentation of the DART.

STRUCTURES

One of the most important aspects of any aircraft design is the structural integrity of the craft. To determine the integrity of the plane, the loads must be identified and calculated. From the loads, the shear forces and moments can be determined, and then finally the levels of stress can be calculated. These steps must be taken for the wing, canard, tail, and fuselage.

The loads can consist of aerodynamic loads, weight of the actual structure, and weight of other loads, such as fuel acting on the structure. The forces acting on the wing provide a good example of the method. The lift distribution over the span of the wing is basically elliptical and can be estimated. Using this distribution along with the geometry of the wing, an estimation of the aerodynamic force on the wing can be obtained. This load can be multiplied by a load factor, 2.5 for this design, to simulate the maximum force encountered. The weight of the fuel stored in the wing and its distribution throughout the wing is known. Also, the weight of the wing with respect to span can be estimated. Since the weights act against the aerodynamic loads, they tend to reduce the overall load on the structure. These forces are shown in Figure 6.

All of the forces acting on a structure can be combined to determine the overall load acting on the structure. This complete loading is shown in Figure 7. Using standard techniques and sign conventions, the load can be integrated to determine

shear, and the shear can be integrated to obtain the moment diagram. The shear and moment diagrams for the canard, wing, tail, and fuselage are shown in Figures 8 through 11, respectively.

From the moment diagrams, the stress due to bending can be determined. However, the shape and construction of the structure must first be estimated. The construction of the structures on the DART-75 will not vary much from conventional designs. The structures will consist of a relatively thin skin along with stringers to handle most of the bending stress. This construction is nearly approximated by a stiffened beam of skin and stringers, where the skin does not handle any normal stress. The stringers that are used in these calculations were assumed to be rectangular. The stiffened beam approximation and the rectangular stringers tend to make these estimates conservative.

Using these estimations, the stress levels in the stringers can be calculated. The material used for the structural members was 6061-T6 wrought aluminum. This material is widely used in the aircraft industry, and is known to have yield strength of 35,000 psi and an endurance limit of 13,500 psi. The endurance limit is the amount of stress that can be applied to the specimen an indefinite number of times without the specimen breaking. Some of the structural members are designed to have maximum stress levels under the endurance limit. Although this makes for a slightly heavier aircraft it extends the life of the structural members. However, the members that are most important are those

which endure the maximum levels of stress.

From the moment diagrams, the points in the structure which will be exposed to the most stress can be determined. The actual levels of stress at those points can then be calculated. In the wing the maximum stress occurs where the large diamond shaped portion ends. This stress was determined to be about 16,100 psi. This value gives the vital members a safety factor of 2.19. In both the canard and tail the maximum stress occurs at the root of the structure. The maximum stress in the canard is 11,400 psi and in the tail is 13,300 psi. These values correspond to safety factors of 3.07 and 2.63, respectively. The maximum stress in the fuselage occurs near the center of gravity of the craft, and has the value of 7600 psi. This level of stress translates into a safety factor of 4.6. These values for stress are only approximations due to the assumptions and approximations used in the calculations, but are good values for this preliminary design report.

The DART-75 attempts to be as efficient as possible, but structural integrity can not be sacrificed to accomplish the goal of efficiency. A conservatively designed structure requires less maintenance and less replacement of structural members, which tends to reduce operating cost. The structural design of this craft could probably be made lighter, but pressing safety and maintenance demands seem to justify the slight weight penalty.

WEIGHT AND BALANCE

In estimating the weight, a combination of formulae was used from two sources, Torenbeek and Nicolai. The two sources allowed tailoring of the weight calculations to our specific design. Torenbeek's formulae involved a complete method of estimating the total structural weight by dividing the structure into major groups. However, this source did not include formulae for individual components that is necessary for a detailed analysis of the balance. This is where Nicolai's formulae are used. The formulae are older than Torenbeek's, but provide more specific component weight calculation as mentioned before. These two sources combined gave us a good approximation to the weight that is appropriate in this stage of the design.

The formulas are meant for a subsonic transport with all metal, mostly aluminum and light alloy, construction. The coefficients used in the equations are then further explicit for the configuration of our aircraft. For example, medium range and medium passenger, rear fuselage pylon-mounted engines, T-tail type empennage, and other smaller details.

The weight is divided into major structural groups and individual groups of components within the major groups. The values of the parameters used in the calculations are outlined in the performance section. The exact formulas used for the calculations are shown and discussed next with the results shown in Table 1. All equations and parameters are in English units.

For the fuselage, the weight is mostly a function of the shell area.

$$W_{fuse} = 0.021 \sqrt{V_D(\frac{l_t}{2D})} S_G^{1.2} \quad . \tag{1}$$

S_G is the gross shell area of the entire body with D being the diameter of the largest cross-section. V_D is the design descent speed and l_t is the moment arm of the tail. Twelve percent of this figure is added to account for the pressurized cabin and fuselage mounted engines.

For the wing group, the weight is largely determined by loads that will be placed upon them and their area. The equation is

$$W_{wing} = 0.0017\ WZF\ b^{0.75}[1+(\frac{6.25}{b})]\ N^{0.55}\ (\frac{b\ S}{t_r})^{0.3} \quad . \tag{2}$$

WZF is the maximum zero fuel weight or the maximum total ramp weight minus the weight of the fuel. S and b are the reference wing area and the wing span, respectively. The maximum thickness of the root chord is represented by t_r and N is the ultimate load factor experienced by the aircraft.

The next group is the undercarriage.

$$W_{uc} = [A+B\ W_T^{0.75}+C\ W_T+D\ W_T^{1.5}], \tag{3}$$

where A,B,C, and D are coefficients for the main and nose gear depending upon the configuration the aircraft. For the nose,

A=20, B=0.10, C=0, and D=2x10^{-6}. For the main landing gear A=40, B=0.16, C=0.019, and D=1.5x10^{-5}. W_T is the maximum takeoff weight as determined by the performance calculations. In Table 1 the weights of the nose gear and the main gear are shown as W_{ng} and W_{mg} respectively.

The weight of the empennage is calculated from

$$W_{tail} = 0.4\,[N\,S_{tail}^2]^{0.75} \quad . \tag{4}$$

It is seen that the area of the horizontal portion of the tail and the load factor are all that are needed to determine the weight. It is expected that this figure will comprise 3.5 to 4% of the empty weight for the aircraft. The same equation was used to calculate the weight for the canard, W_{canard}, in our design. However, the coefficient 0.4 was changed to 0.2 since the canards are only two horizontal pieces extending from the sides of the forward fuselage and there is no vertical part to the canard. 20% of these weights were subtracted to account for our use of composites in the tail, canard, and flight control surfaces.

The surface controls weight was calculated from the formula,

$$W_{sc} = 0.64\ W_T^{2/3} \quad . \tag{5}$$

This is entirely a function of the takeoff weight. The takeoff weight will determine the size of the control surfaces through the aerodynamic analysis. The size in turn will determine how much of a control surface is needed and therefore the weight. 20% was added since our design will incorporate forward flaps and

other high lift devices.

Eqs.(1-5) were all obtained from Torenbeek's method. The weights of the fuselage, wing, undercarriage, empennage and canard, and the surface controls calculated from Eqs.(1-5) were compared to the weights for the same groups calculated from Nicolai's formula. The values were 0 to 7% higher than those found from Torenbeek's. This is expected since the seven year difference in the publishing of the books may have created a better analysis due advancement in technology during that time span and is even more justified for the time span since Torenbeek's publishing leading up to the current date.

The rest of the equations listed in this section are weight estimation formula for some typical components common to a medium range transport. All were found from Nicolai's book. First are the equations for the fuel system components. This comprises self-sealing bladder cells, backing and supports, a dump and drain system, and a C.G. control system including transfer pumps and monitor. The equations respectively are:

$$W_{bc} = 41.6\ [(F_g)x10^{-2}]^{0.818}. \tag{6}$$

$$W_{bs} = 7.91\ [(F_g)x10^{-2}]^{0.854}. \tag{7}$$

$$W_{dd} = 7.38\ [(F_g)x10^{-2}]^{0.458}. \tag{8}$$

$$W_{cgsys} = 28.38[(F_g)x10^{-2}]^{0.442}. \tag{9}$$

F_g is the total fuel capacity in gallons. The fuel system weight, $W_{fuel\ sys}$, is the sum of Eqs.(6-9).

For the engine controls, the following formula was used.

$$W_{engco} = 0.686\,(l_f\, N_{eng})^{0.792}\ . \qquad (10)$$

l_f is length of the fuselage and N_{eng} is the number of engines on the aircraft, two for our design. The weight of the engine itself, W_{eng}, was found from the data on the development of the engine. Other associated items with the engines are the nacelles, pylons and starting system. The equations used for the weights of these components are shown here.

$$W_{np} = 0.065\,(W_T)^{2/3}. \qquad (11)$$

$$W_{ss} = 38.93\,[(N_{eng}\, W_{eng})\, x10^{-3}]^{0.918}. \qquad (12)$$

The starting system weight is for an electrical-type operation. Again, 20% of the weight of the nacelle was taken away for composite use in that area. Eqs.(10-12) were added together for the total accessory parts needed for the operation of the engine as $W_{eng\ acc}$ shown in Table 1.

Other items to consider for estimating the weight include the furnishings. The weight of the flight deck seats was determined from the equation

$$W_{fds} = 54.99\ N_{fds}\ . \qquad (13)$$

N_{fds} is the number of flight deck seats. This aircraft is

designed to be operated by a pilot and co-pilot. So N_{fds} is two for this case. The passenger seat weight were calculated from

$$W_{ps} = 32.03\ N_{pass}\ . \qquad (14)$$

The air conditioning/pressurization system weight is combined

$$W_{ac} = 469.3\,[V_{pr}\ (N_{crew} + N_{pass})\,x10^{-4}]^{0.419}. \qquad (15)$$

with the anti-ice system and is related by this formula, N_{crew} is four which includes the two aircrew and two flight attendants. V_{pr} represents the occupied or pressurized volume.

The weight category of W_{misc} is a sum of all the weights of other components found in a transport such as ours. These are items such as: emergency oxygen system, flight and engine instruments, electrical system, cabin windows, baggage handling provisions, food and water provisions, and lavatory provisions. The equations were found in Nicolai's book and are not repeated here for the following reason: these items are such that their weights are evenly distributed over the entire aircraft, or can be designed that way, and are considered not to have a major affect on the balance analysis.

The weight of the avionics was found from Table 8.1 in Nicolai's book. This table lists common weights of typical aviation electronic equipment. The weight of the equipment that are common for a commercial transport were obtained from this table and added. The total weight was rounded up to 2000 lb for a conservative estimate and since this design will have more

avionics than that shown in the referenced table. This is typical of today's more sophisticated aircraft (e.g., fly-by-wire, GPS and other satellite communications, advanced, more informing electronics) than those produced before 1975 when the table was printed.

Using a weight per person of 175 lb and 50 lb of baggage per passenger, the maximum payload weight, Wpayload, was found by multiplying 79 persons times 175 and adding that to total baggage weight of 75 times 50. The figures of 175 and 50 were obtained as an industry standard average for formulating payload weight. A value of 12 lb/ft^3 was found from Torenbeek's book for the average specific density of baggage. This made possible the calculation of about 320 ft^3 that is necessary for baggage stowage. Another industry standard of 6.5 lb/gal for JP-4 fuel was used with the total fuel held of 3400 gallons to calculate the fuel Weight. This weight plus the payload and empty weight give the total maximum ramp weight, MTRW, of the aircraft. The empty weight is the sum of the all the group and component weights shown as W_e in Table 1.

The balance analysis was done with reference to Torenbeek's book. The calculation was done by breaking down the aircraft into major components and subcomponents with a simple center of mass technique. The equation for the center of gravity in the longitudinal direction is

$$\bar{x} = \frac{\sum (\bar{x}_i \, W_i)}{\sum W_i} \qquad (16)$$

The same approach is used for the vertical center of gravity distance reference to the ground while the aircraft is on the ground, but x is replaced by z in Eq.(16). The nose of the fuselage was used for the reference datum line while calculating the center of gravity along the length of the aircraft, as seen in Figure 12.

The center of gravity is considered to lie on the centerline of the aircraft. Since this design layout of the cabin includes rows of five seats across, there will be an off-balance due to the passengers and their seats. Three seats in a row will lie on one-half of the fuselage cross-section. The other two seats in the row will be fixed in the other half leaving a deficit of weight on one side of the fuselage. Most transport aircraft with this type of layout make up for the deficit by arranging components to be fixed to deficit side. Once passengers are loaded, their baggage and some fuel are loaded in a way to overcome the off-balance due to the weight of the passengers. This design will follow the same concept. Some of balance setting components might include some of the avionics, powerplant accessories, or reserve fuel since most other components are typically fixed to the configuration.

Different flight configurations had to be examined in order to account for all types of scenarios or events. The configurations looked at represent the extremes of flight configurations. This gives a defined set of center of gravity positions. Two of which are the most fore and aft center of

gravity locations. The difference in the two positions give the center of gravity travel that can occur in flight. The four payload-type configurations are: full load (all passengers and full fuel), full fuel and no passengers (and no baggage), reserve fuel and all passengers, and reserve fuel only. Table 2 shows the figures for each of the configurations.

Torenbeek presented a way to roughly estimate the moment arms of the major components of the aircraft. For the wing, the center of gravity is 42% of the chord from leading edge at 40% semi-span from centerline. The fuselage center of gravity is at 47% of the fuselage length from the nose. The horizontal tail plane and canard c.g. is at 42% of the chord at 38% semi-span from root chord. The vertical stabilizer c.g. is 42% chord from leading edge at 55% of height from root chord. Nacelle c.g.s are 40% of nacelle length from nose of the nacelle added to the distance from the nose of the aircraft to the front of the nacelles. The engine c.g. was found from data on the design of the engine. The surface control system c.g. is at 100% MAC from the leading edge of the MAC excluding auto pilot.

The distances for the landing gear and furnishings were made by educated guess based on the definition of our design. The center of gravities for the fuel, baggage, avionics and other accessories were placed to satisfy stability requirements.

STABILITY AND CONTROL

The subject of stability and control deals with how well and aircraft flies and how easily it can be controlled. These factors are especially important for a commercial transport because of the passenger comfort requirements. A passenger aircraft must adjust quickly and smoothly to perturbations in the atmosphere and changes in flight conditions.

There are many criteria which must be satisfied for an aircraft to be considered statically stable. Using one of the Army's Missile Aerodynamic Design Programs written by William David Washington in 1980 and modified by Dr. John E. Burkhalter of Auburn University in 1990, many stability parameters were determined. These values are given in Appendix A. From this data and hand calculations, the pitching moment coefficient, drag coefficient, and lift coefficient were plotted versus angle of attack and are shown in Figures 13, 14, and 15. One criterion for the DART to be stable is that the moment curve slope must be negative. The moment curve slope for the DART is approximately -4.304 per radian. The numbers obtained from the design program are approximate because it was necessary to estimate the wing shape because the program was unable to accept a cranked wing configuration. A stable aircraft must also be able to be trimmed. The Y-axis intercept of the pitching moment curve must be positive and was determined to be 0.152 for the DART. The following equation is used by the design program to determine the moment coefficient slope.

$$C_{m_a}=a_{wb}[h-h_{n_{wb}}-V_H\frac{a_t}{a_{wb}}(1-\frac{\partial \epsilon}{\partial \alpha})+V_c\frac{a_c}{a_{wb}}(1-\frac{\partial \epsilon}{\partial \alpha})] \qquad (17)$$

Another important stability parameter is the stick fixed static margin. The static margin must be positive for a stable aircraft. The static margin can be determined from the following equation using the design program output.

$$\frac{X_{cp}}{c}=\frac{-C_{m_{a_{cg}}}}{C_{N_{a_c}}+C_{N_{a_w}}+C_{N_{a_t}}} \qquad (18)$$

The static margin for the DART at cruise was found to be 2.73 feet or 34 percent of the mean aerodynamic chord. Acceptable values for the static margin for commercial transports range from 25 to 50 percent of the mean aerodynamic chord. This means that the center of pressure is 2.73 feet behind the center of gravity and therefore the DART is statically stable.

The maneuver margin is another important stability parameter. The maneuver point should be behind the center of gravity. The maneuver margin was determined to be 10.2 feet from the following equation:

$$h_m=h_n+\frac{h}{\mu}a_t\frac{l_t}{c}V_H \qquad (19)$$

Therefore, the maneuver point at cruise for the DART is 10.2 feet behind the center of gravity.

The stability characteristics about the yaw and roll axes are closely coupled. The upward sweep of the wings generates a dihedral effect. The dihedral effect produces restoring forces

and moments in the yaw and roll directions. A dihedral angle of about 8 degrees is necessary in order to reduce the body interference factor on the dihedral effect.

The DART-75 will use three control surfaces. Elevators will be on the tail to control pitch and altitude changes. Due to the close coupling of the yaw and roll controls, the rudder mounted on the vertical tail plane and the ailerons on the wing are interdependent. These surfaces will give adequate response to perturbations and sideslip forces. These controls are conventional in design and should give the DART-75 handling qualities similar to other regional jets. Dynamic analysis is not within the scope of this report given the time and resource constraints. When a model is produced, further analysis may be done.

PERFORMANCE

The DART's performance data was obtained through the use of two main sources, Fundamentals of Flight, by Richard Shevell, and UsAir Operations Chief Engineer Mike Pulaski. The drag was calculated by using Methods For Estimating Drag Polars of Subsonic Airplanes by Jan Roskam, Professor of Aerospace Engineering. Several things were needed for the calculation of the drag polar, as seen in Table 3. From this method the drag polar is

$$C_D = .02167 + .0301\ C_L^2 \qquad (20)$$

for the clean configuration and

$$C_D = .065341 + .0309\ C_L^2 \qquad (21)$$

for the dirty configuration.

A plot of the drag polar is shown in Figure 16. The coefficient of lift has a maximum value of 1.75 for the clean configuration and 2.2 for the dirty configuration. Using the calculated drag polar a variety of information is found. The first of these is the DART's flight coefficient of lift. The coefficient of lift for maximum lift over drag was found to be .75. Figure 17 shows the Mach number plotted against the drag coefficient at various heights. The first plot is at standard atmospheric conditions. The next is at 10,000 feet and the third is at a flight altitude of 30,000 feet.

The next calculation involved determination of the flight

speed. Depending upon the choice of the coefficient of lift the flight speed will vary. The equation that determines the velocity at level unaccelerated flight is:

$$V = \sqrt{\frac{2w}{\rho S C_L}} \qquad (22)$$

Through this simple formula the velocity at any coefficient of lift may be determined. Upon the usage of the maximum lift coefficient the stall velocity is obtained. The flight velocity was determined through the use of the coefficient of lift for the maximum lift over drag of .75. The maximum, minimum, stall and flight velocities are graphed against the altitude in Figures 18. The maximum and minimum flight velocity was calculated through the use of;

$$V = \left[\frac{2}{\rho}\left[\frac{F}{2C_{D_o}}\frac{\rho}{\rho_{sl}} +- \sqrt{\left(\frac{F}{2C_{D_o}S}\right)^2 - \frac{kw^2}{C_{D_o}S^2}}\right]\right]^{\frac{1}{2}} \qquad (23)$$

The first graph of the altitude versus the velocity was determined by letting the thrust vary linearly with altitude. The thrust was determined from the type of engine that was chose for the DART. Once a thrust was assumed then the minimum and the maximum velocities were determined and plotted. Also shown is a plot of the altitude versus the thrust as seen in Figure 19. The minimum thrust required and the flight thrust at cruise altitude is plotted against velocity in Figures 20. Figures 21, 22, 23 show the thrust available and the thrust required versus the velocity. These figures are shown at sea level, 10,000 feet, and

30,000 feet. Appendix B shows the data obtained through the calculations of thrust and velocity. The stall velocity was also plotted against altitude in Figure 24.

The range was determined through the use of a rough estimation range equation

$$R = \frac{1.675}{tsfc}\frac{1}{\sqrt{\rho S}}\left(\frac{C_L^{\frac{1}{2}}}{C_D}\right)\left(\sqrt{w_i}-\sqrt{w_f}\right) \qquad (24)$$

In calculating the range the maximum weight that the aircraft is able to carry was used. The final weight W_f includes fuel reserves. Upon the calculation of the range the DART was found to have a range of 1208.69 miles. This calculation fit very well with the mission profile that was stated in the earlier proposal. The calculation of the endurance was along the same lines as that of the range calculation. By knowing the engine's specific fuel consumption and the weight of the fuel then the endurance of the flight was determined to be around five and a half hours. This calculation was done without the consideration of the fuel burned during take-off. If taken into account then the maximum endurance is calculated to be around five hours.

The DART's ground roll for takeoff was found to be approximately 3463 feet. This was done at full load at maximum thrust. The total take off distance was calculated to be 5591 feet. These calculations were done with the consideration under FAA regulations the aircraft has to have enough room to clear a 35 feet obstacle and also be 115% bigger than calculated field

distance. Also calculated under FAA regulations was the landing distance. Through comparison of various aircraft and their total landing field length and equations supplied by Fundamentals of Flight. The landing field was determined to be 7651 feet. Thus the performance of the DART does indeed fit the original proposal of a quick multi-stop spoke to spoke or spoke to hub regional aircraft.

The DART climb performance is comparable to any other regional aircraft. With the mission profile, as shown in Figure 25, the DART will climb from sea level to around 75% of cruise altitude in approximately 10 minutes. This will be at an initial climb angle of between 8 and 14 degrees at a climb rate of between 3400 to 5500 feet per minute. After reaching the 22500 foot level, the DART will begin to level off to a more relaxed climb angle ranging from two to five degrees. The climb rate will then be between 1000 and 3000 feet per minute. Another 5 minutes and the aircraft will be at a cruise altitude of 30,000 feet.

PROPULSION

Due to the multi-faceted role of regional aircraft, a propulsion system designed for this aircraft must be able to handle many different flight conditions. The engines will not be the best design for any one situation, but they should be a good compromise for the situations in which the airplane is to be used. This aircraft is intended to be used in short multi-hop spoke to hub operations and/or in medium range point to point operations. A short multiple flight spoke to hub operation consists of three to four landings at airports near one hundred miles apart with a final landing at a major hub airport like Hartsfield International or Memphis International. A medium range point to point operation is one that consists of a flight between two airports approximately five hundred to six hundred miles apart. An example of a point to point flight would be a trip from Hartsfield International Airport in Georgia to San Antonio International Airport in Texas.

To achieve this goal, three engine configurations were explored. The first was the very high bypass turbofan engine. The second consideration is the propfan engine. Lastly, the Counter-Rotating-Integrated-Propfan or CRISP engine was analyzed. Each engine should produce between 10,000 and 15,000 pounds of static thrust, be able to provide reverse thrust, and should comply with aircraft noise regulations.

The turbofan engine has been around for many years and it has proven to be very successful. The turbofan engine has been

selected for consideration primarily due to its proven technology. Since there have been so many aircraft designed for turbofan engines, there is an abundance of research that has already been conducted in this field. Trends in turbofan engine design are to increase the engines bypass ratio rather than improve the engines core design. The increase in bypass ratio allows the engine to produce the same thrust with a smaller thrust specific fuel consumption and with less noise. Some more advantages of the turbofan design are: low initial cost and maintenance, lower operating weight for the aircraft due to lower engine weight, and better load distributions for wing mounted engines.

Propfans are a relatively new engine design. A propfan engine consists of a core engine identical to a turbofan. However, the engine uses one or two cascades of propeller blades to produce a higher bypass ratio than a ducted fan. The propeller is a more efficient propulsion device than a fan. Some of the advantages allowed by the use of a propfan are: low specific fuel consumption, efficient thrust reversing, a rear engine mounting allows for a clean wing, and a larger amount of static thrust for the same cruise thrust. However, there are also penalties for these advantages. A propfan engine weighs about thirty-eight percent more than the same turbofan engine, is extremely loud due to the unshrouded propeller blades, and the Federal Aviation Administration has not approved mounting this type of engine under the wing. The FAA's reluctance is due to

the risk of a blade breaking off and passing through the passenger compartment. Since engine weight is usually between ten and fifteen percent of total aircraft weight the difference could make a substantial change in aircraft efficiency. A comparison of a turbofan and propfan engine designed for a regional class aircraft is shown in Figure 26.

The last engine design considered for the regional aircraft design was a Counter-Rotating-Integrated-Propfan (CRISP) engine. A CRISP engine has the same core engine as the two other engines, two cascades of counter rotating propellers, and a cowling to shroud the propellers. This design should provide the advantages of both the propfan design and the turbofan design. The advantages of the CRISP engine deduced from the turbofan engine are: conventional wing mounting, high cruise speeds, noise reduction, and blade containment. As said earlier below wing mounting of the engines allows for better balance of the aircraft and easier access during maintenance. Higher cruise speeds can be attained by adjusting axial mach numbers for cruise speeds. Noise reduction is provided by the cowling. Lastly, blade containment will be an advantage, because the FAA would probably be more apt to allow the wing mounting of the engine. The characteristics derive from the propfan are: low specific fuel consumption and excellent reverse thrust capability. The lowered specific fuel consumption is achieved by using very efficient propellers and a bypass ratio that is approximately twice that of a turbofan. The reverse thrust is also provided by the

propellers, which can be turned to a negative angle of attack. However, like the propfan engine the CRISP engine has some draw backs. A CRISP engine is going to be heavier than a turbofan engine of the same thrust and the technology used to develop the CRISP engine design has not yet been proven.

From analysis of the three options, it was deduced that a high-bypass turbofan engine would be the best option. The turbofan engine is designed with proven technology. Therefore, the turbofan engine displays a greater degree of reliability than the propfan or the unproven CRISP engine. The turbofan cannot be designed with as high of a bypass ratio as the propfan or the CRISP engine. However, the decreased weight and lower maintenance costs will far out weigh the cost due to higher fuel consumption.

The engine used on the aircraft will be capable of producing 12,500 pounds of static thrust and will produce 2,500 pounds of thrust at 30,000 feet and a mach of .6. The thrust specific fuel consumption (TSFC) of the engine should be approximately .6293 (lb/hr)/(lb/F), this value was calculated using a computer program that will be discussed later in the paper. To achieve such a low TSFC an engine will need a bypass ratio from about 7 to 10. The weight of the engine will be around 1800 pounds, a length of 7.3 feet and a diameter of 5 feet.

Most engines that are put on higher performance aircraft are d-rated. In other words the engines can produce greater power when needed than the actual design power required for any flight

situation. Therefore, the actual engine put on the DART-75 will probable be capable of producing 15,000 to 20,000 pounds of static thrust. This increase of power would allow for greater single engine takeoff and climb performance and would also allow the airplane to climb to a higher altitude in case it needed to avoid thunder storms. The increase in thrust to 17,500 pounds would require an engine that weighs 2,535 pounds, is 8.32 feet long, and is 6.36 feet in diameter. The added increase in weight would only change the total aircraft weight by 1,570 pounds, which would be an increase of only 2.0 percent. However, the increase in static thrust would change the single engine thrust to weight ratio on takeoff from .156 to .22.

The weight, length, and diameter of the engines presented above were calculated using the following equations.

$$W = 0.084\ (thrust)^{1.1}\ e^{-0.045\ BPR} \qquad (27)$$

$$L = 2.22\ (thrust)^{.4}\ M^{.2} \qquad (28)$$

$$D = 0.393\ (thrust)^{.5}\ e^{0.04\ BPR} \qquad (29)$$

These equations were obtained from Daniel P. Raymer's book Aircraft Design: A Conceptual Approach page 196.

The calculation of the example engine was done using the ONX program. This program was derived from the book Aircraft Engine Design written by J.D. Mattingly, W.H. Heiser, and D.H. Daley. The program allows the engineer to input mach number, altitude,

atmospheric conditions, bypass ratio, burner can temperatures, and component efficiencies. The program then calculates the engines mass flow rate, thrust, and thrust specific fuel consumption. The burner can temperature was estimated at 3000°R. The fan pressure ratio is 1.4 and the compressor pressure ratio is 39.0. These values were derived by iterations done with the ONX program. A total of approximately 200 different bypass ratios, fan and compressor ratios were used in the program before the one that produced the lowest thrust specific fuel consumption was found. The engine is also based on the two nozzle non-mixing design.

A bypass ratio of 9.6 was chosen because it proves to be the highest bypass ratio that can be obtained using a standard fan and still be able to keep the engine flow stable. A higher bypass ratio can be obtained. However, to keep the engine flow stable, a fan cascade with variable pitch fan blades would be required. This design would require a significant increase in engine weight and would decrease the reliability of the engine. Therefore, it was determined that the simpler design would satisfy the airplane operators needs better than the variable pitch fan blade design.

The engine will be capable of reverse thrust using ballistic reversers. The failure of ballistic reversers is known to be very unlikely. In fact, there has never been a recorded failure of the clamshell type reverser. The only other option for thrust reversing is available on the propfan, CRISP, and variable pitch

fan design of a turbofan engine. This option is to turn the blades in such a way as to give them a negative angle of attack. Reversing thrust in this manner is more efficient than in the ballistic way but it would once again add unwanted weight and complexity to the engine design.

Currently, the high bypass turbofan is the most sensible choice for propulsion. In years to come, more reliable, lighter, and proven high bypass ratio engines will be available. These engines will allow aircraft to have much higher thrust to weight ratios with an extreme decrease in TSFC. The propfan, CRISP, and high bypass turbofan engines will be the choice of the future. However, until advances can be made on these engines, they do not make a wise choice for an airplane that is being designed for immediate production. If the engines become available during the production life of the DART-75, a modification can be made to the basic airplane and the advantages of the new engines can be applied.

DISCUSSION AND CONCLUSION

The DART-75 design does indeed make for a better and more modern, efficient aircraft. The structural design though unique is indeed very efficient as seen through the calculations of performance and stability. Even though the structures do indeed make for a more efficient aircraft they could still be improved upon. With more time, closer inspection upon the effect of more sweepback upon the wings could have been investigated as well as a smaller tail.

The original design had to be modified several times to include such small items as how much room to allow for the gate to be rolled up to the door. The decision to use a five abreast seating section was made due to the stability factor. If four abreast had been the design, the airplane's main fuselage would indeed be too long to maintain stability very easily.

The DART's performance proves to fit fairly well with the mission profile. The drag calculation, though done by hand, proved to be reasonably accurate, compared with those found through a program. By comparing the calculated values with those values that are known for today's aircraft, reasonable results were achieved. More calculations could have been done with the performance for more altitudes and more varied flight conditions. But, to allow for the calculation of as many performance parameters as possible the basic performance parameters were done at sea level and at cruise altitude.

The drag calculated at various mach numbers could have been

improved if worked upon. The landing and take-off field lengths though not as good as hoped for, originally 3,900 feet, are very respectable and compare well with any regional aircraft in existence today. The range and endurance are very respectable and indeed make for a very good quick aircraft.

The actual material make up of the DART will consist mainly of aluminum. However, some composites will be used to construct the top of the wings, horizontal tail, canard, and parts of the fuselage. The determination of the type of composite used, whether graphite epoxy or fiberglass, would require time for further investigative analysis.

The cost of the DART-75 was first estimated at over 30 million dollars per plane. This cost seemed perhaps too high to be competitive. Research into the cost of aircraft resulted in a change of this impression. The new Canada Air Regional Jet costs about 18 million dollars per plane, and only carries 50 passengers. This cost along with other aircraft costs are shown in Figure 27 plotted against the number of passengers. Using this simple graph we can determine that a 75 passenger craft would cost about 28.5 million dollars. Another estimation method uses cost per passenger, which is plotted versus number of passengers in Figure 28. This method suggests a total cost of 30 million dollars. In light of these estimations, the cost of DART-75 seems reasonable, but is slightly higher than desired.

The cost of the DART-75 was estimated using the DAPCA IV model of aircraft cost. In this method, a factor representing

the amount of composite materials used has to be chosen. A slight reduction in this number results in a considerable decrease in cost. By using slightly less composite materials, the cost of the DART-75 can be reduced to about 28 million dollars. The weight of the craft will not be greatly effected, since the level of composites originally chosen was not reduced greatly. This cost should make the DART-75 very competitive on a cost basis.

SUMMARY

The regional aircraft currently available are old and inefficient. A new regional transport could take over the regional market. The DART-75 is the proposed new regional transport with single class accommodations for seventy-five passengers and a crew of four. The DART-75 can achieve this type of success through its efficiency, excellent multi-role capability, advanced general design, and competitive cost.

The efficiency of the DART-75 is increased in many ways. The use of a canard gives the craft three lifting surfaces, and should increase efficiency. Lightweight aluminum alloys and composite materials reduce weight, and therefore reduce the power required. The careful selection of engines satisfy the craft's power requirements while maximizing efficiency. Other factors such as advanced avionics can further increase efficiency.

The DART-75 will be capable of point to point, hub feeder, as well as shuttle type services. The wing shape, decreased weight, and efficient engines combine to yield good short field performance, excellent range, and competitive cruise speed. These factors make the DART-75 a very versatile craft that will appeal to many airlines for different types of missions.

It has also been demonstrated that the DART-75 has a sound design, considering many factors. Major concerns such as, structural integrity and stability of the aircraft have been addressed. Also, many other concerns that seem less vital have been investigated. These factors include, access of the ground

support crew, comfort of the passengers, location of baggage, and other factors too numerous to mention. With the inclusion of so many factors, it can be deduced that the basic design of the DART is sound.

The expense of an aircraft can be a deciding factor in its success. A revised cost estimate demonstrates that the DART-75 can be produced at a competitive price. The final cost per aircraft would range from about 18 million dollars to 28 million, depending on the number of aircraft produced. This cost has been shown to be quite competitive.

The DART-75 could dominate the weak competition in the regional aircraft market with its efficient, multi-role design. As this proposal demonstrates, the DART-75 can achieve its goals while keeping its cost competitive, and reestablish the regional transport as a major part of the aviation industry.

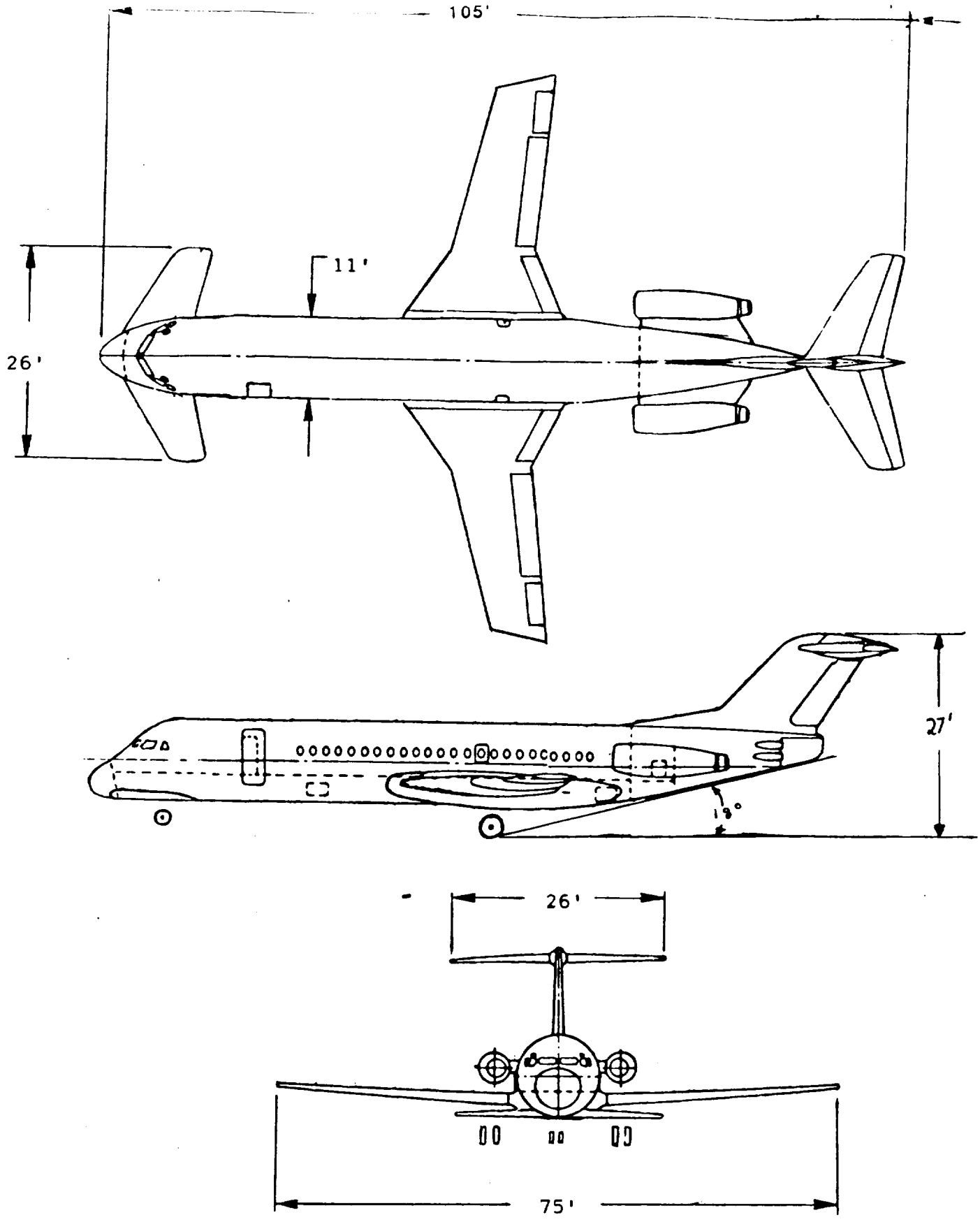

Figure 1: Three View Diagram

Galley

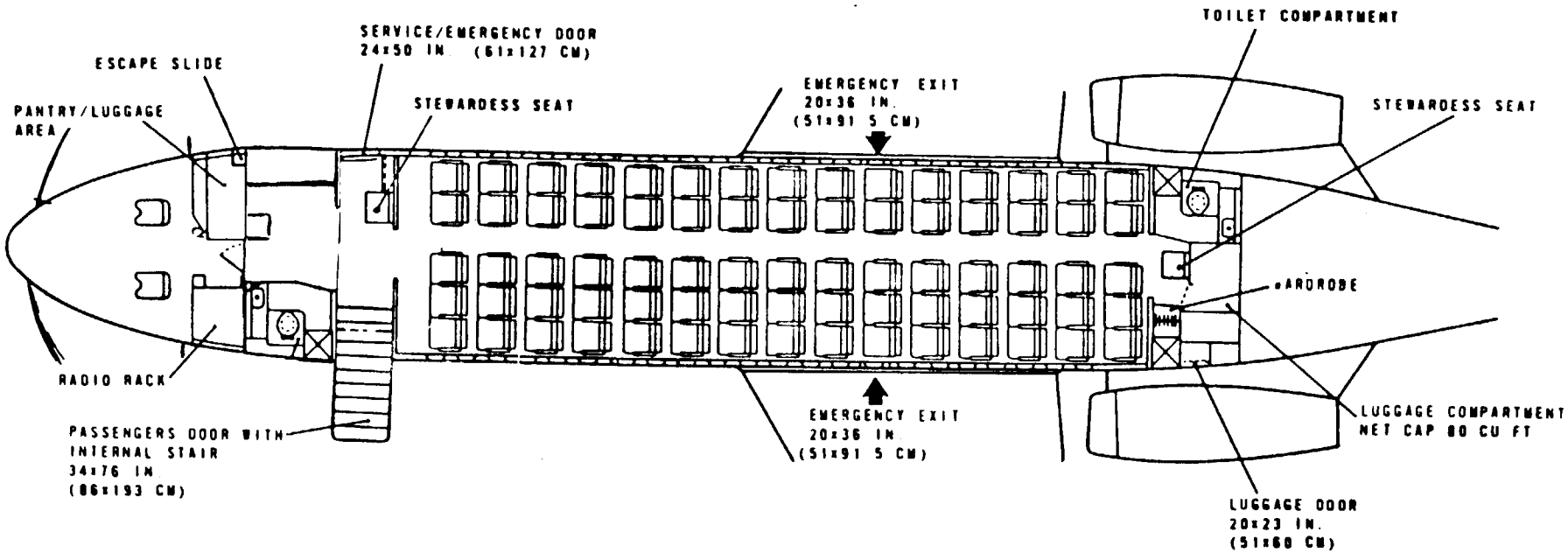

Figure 2: Interior Design

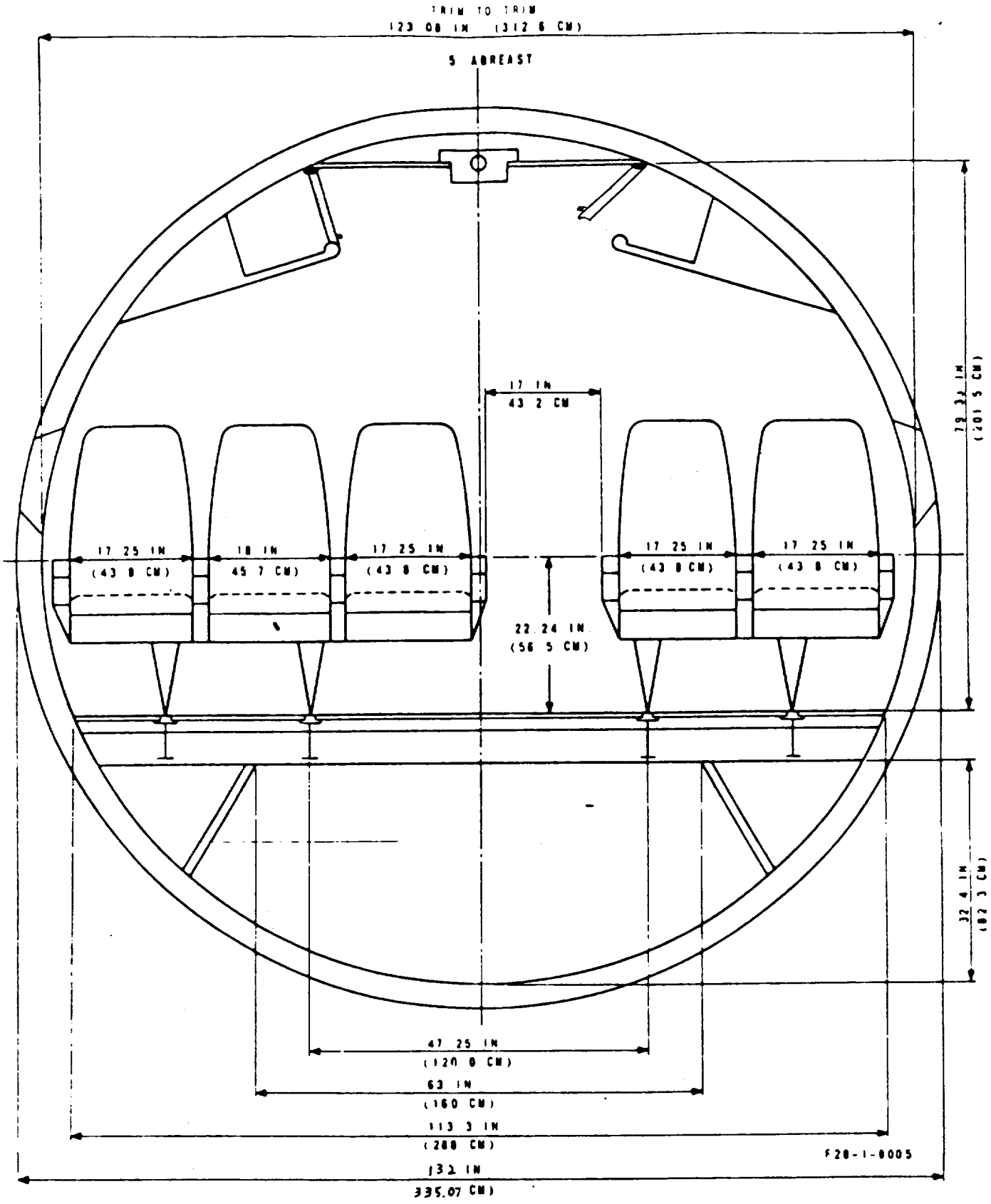

Figure 3: Cross Section of Interior Cabin

EQUIPMENT POSITIONING

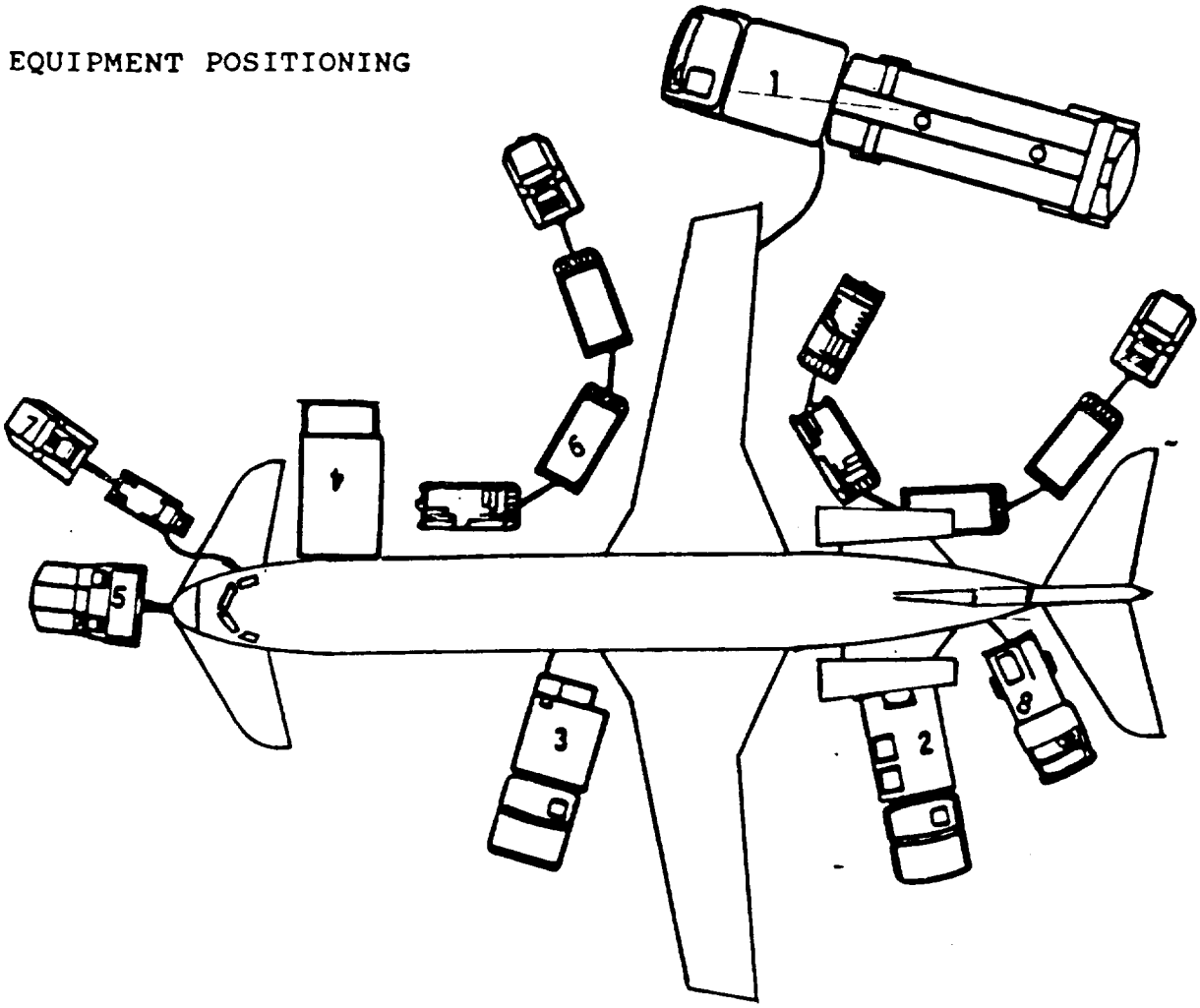

1 - FUEL TRUCK

2 - LAVATORY SERVICE CART

3 - WATER SERVICE CART

4 - CATERING TRUCK

5 - HOUGH TRACTOR (some units can be used for Ext. Pwr.)

6 - BAGGAGE CARTS

7 - GPU (head away form aircraft)

8 - AIRSTART TRUCK

Figure 4: Ground Handling

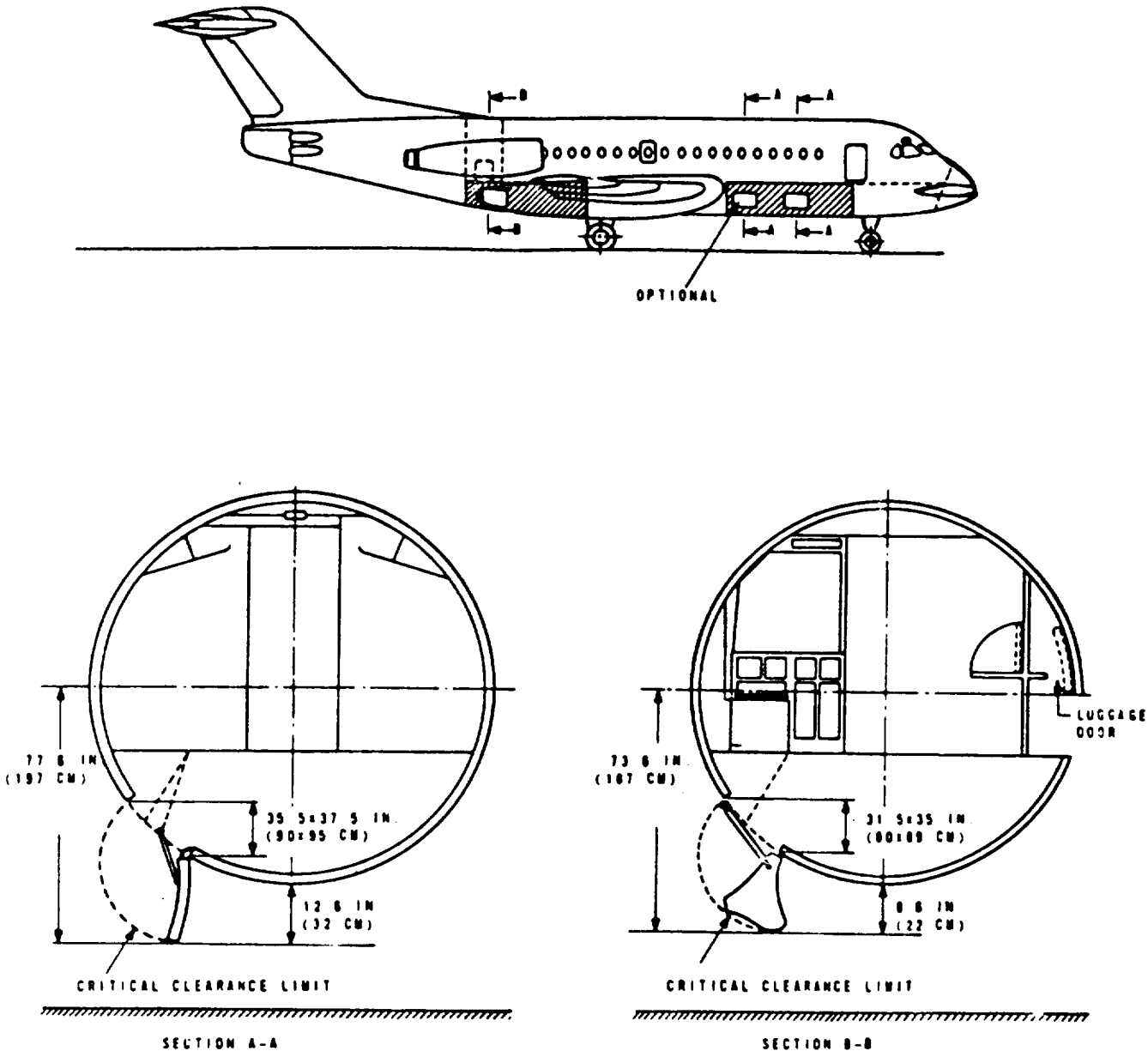

Figure 5: Characteristic Loading

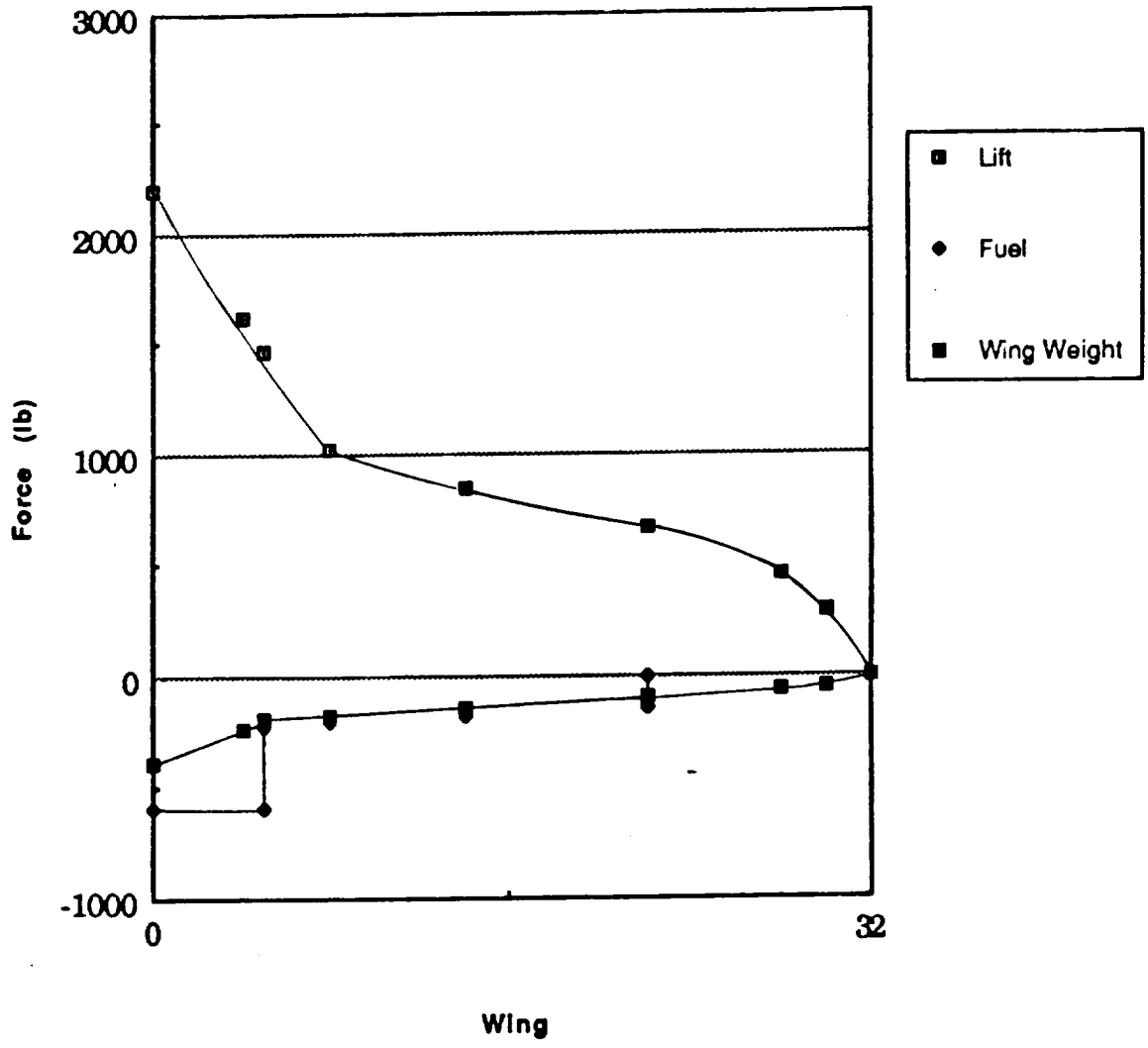

Figure 6: Forces on the Wing

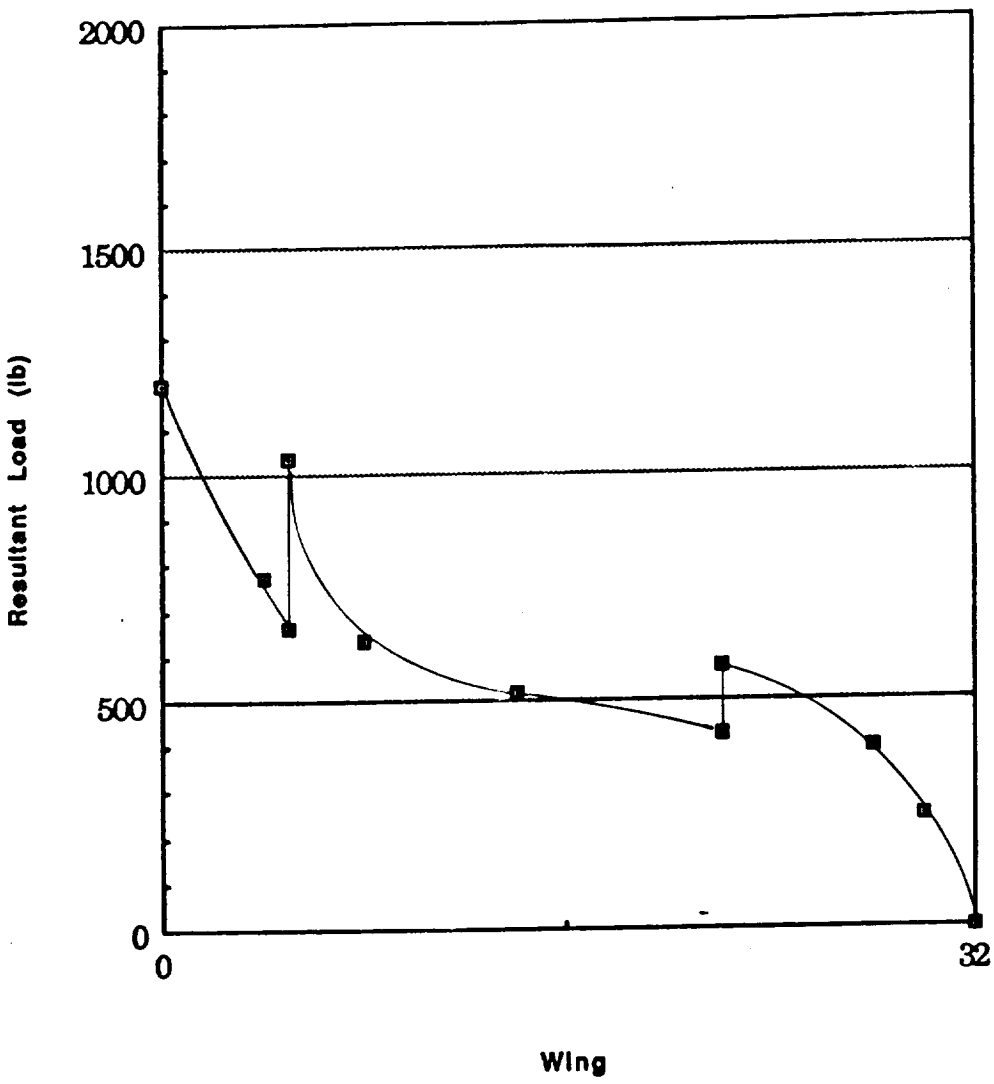

Figure 7: Sum of the Forces on the Wing

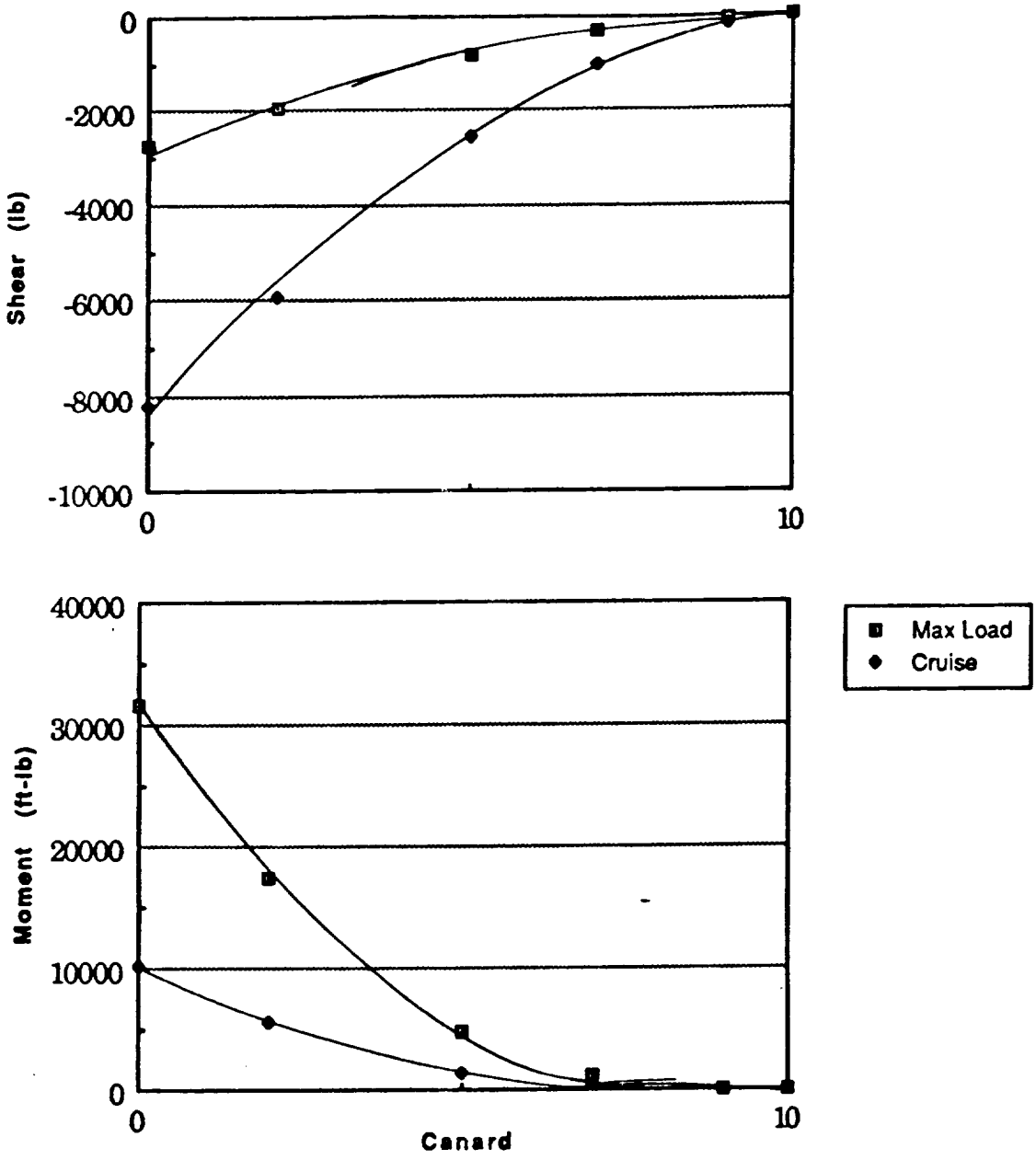

Figure 8: Shear and Moment Diagrams for the Canard

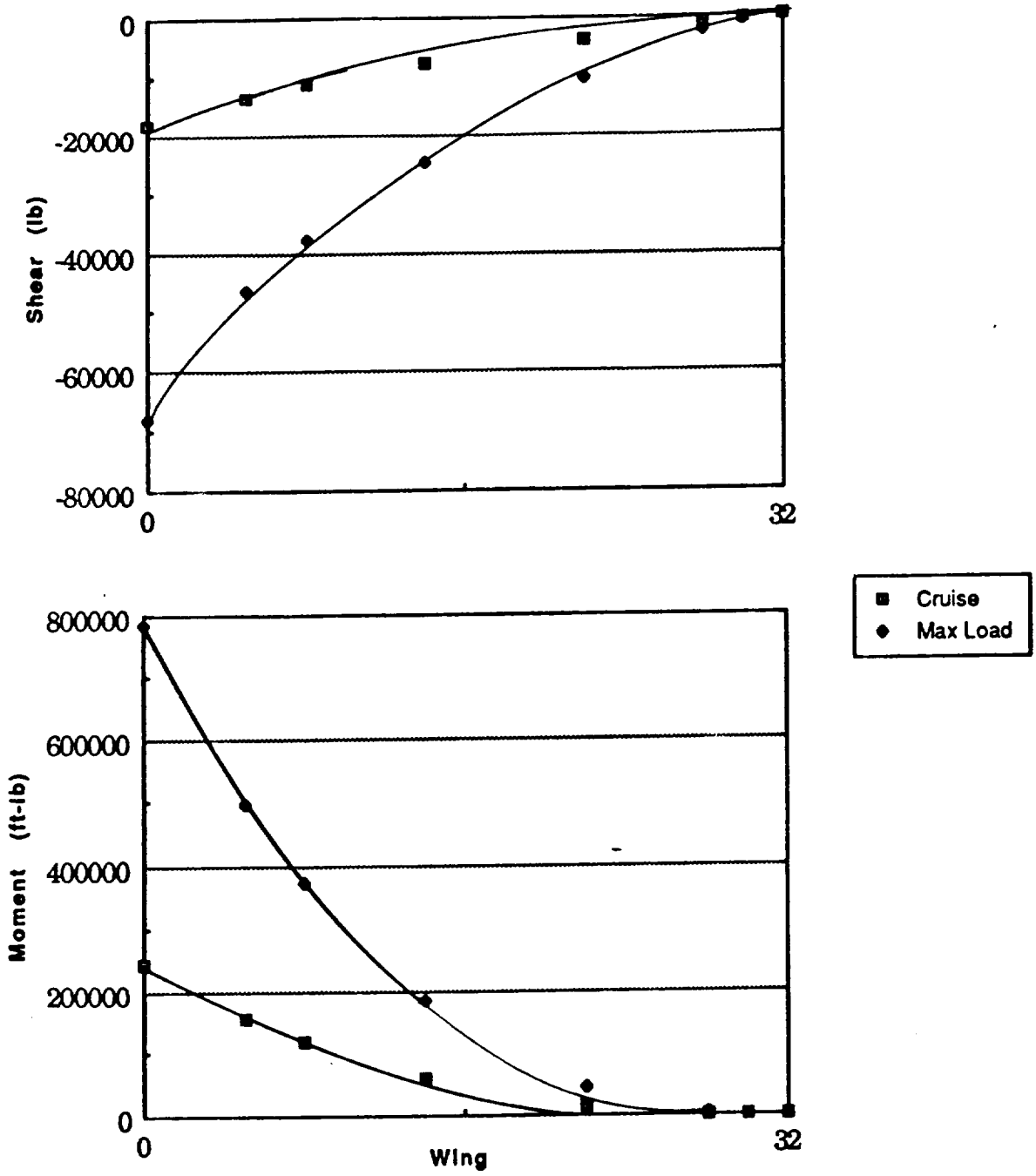

Figure 9: Shear and Moment Diagrams for the Wing

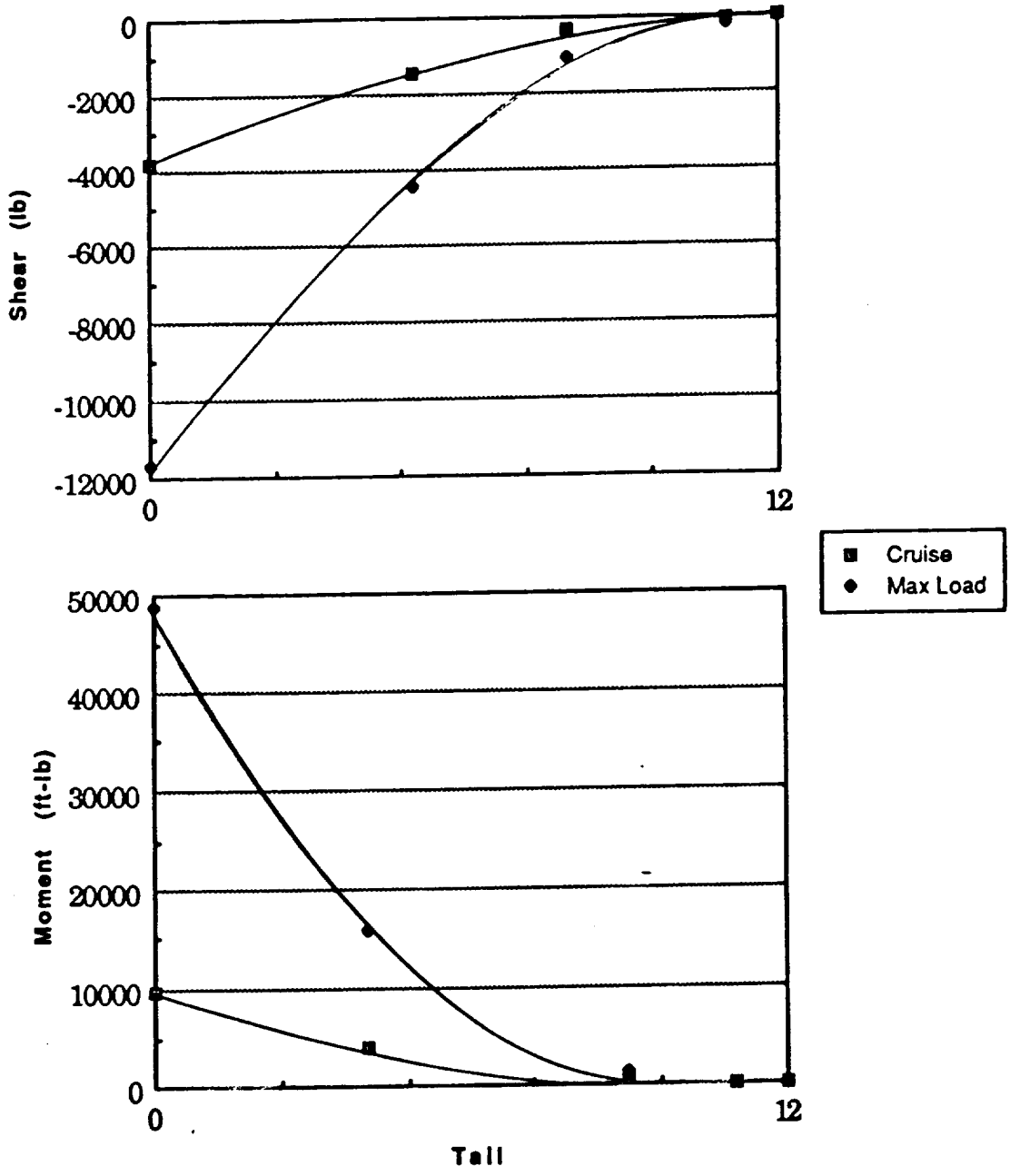

Figure 10: Shear and Moment Diagrams for the Tail

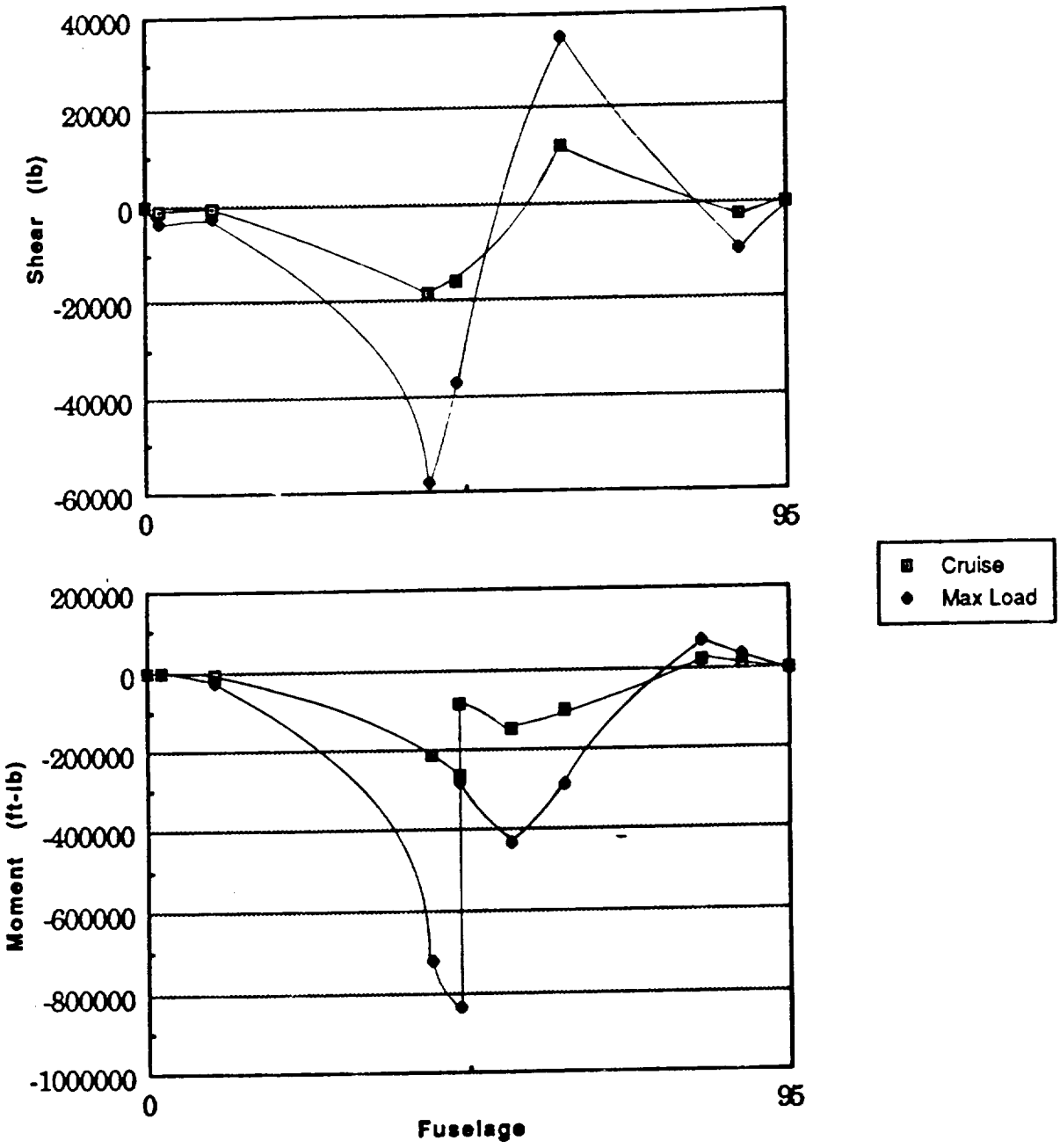

Figure 11: Shear and Moment Diagrams for the Fuselage

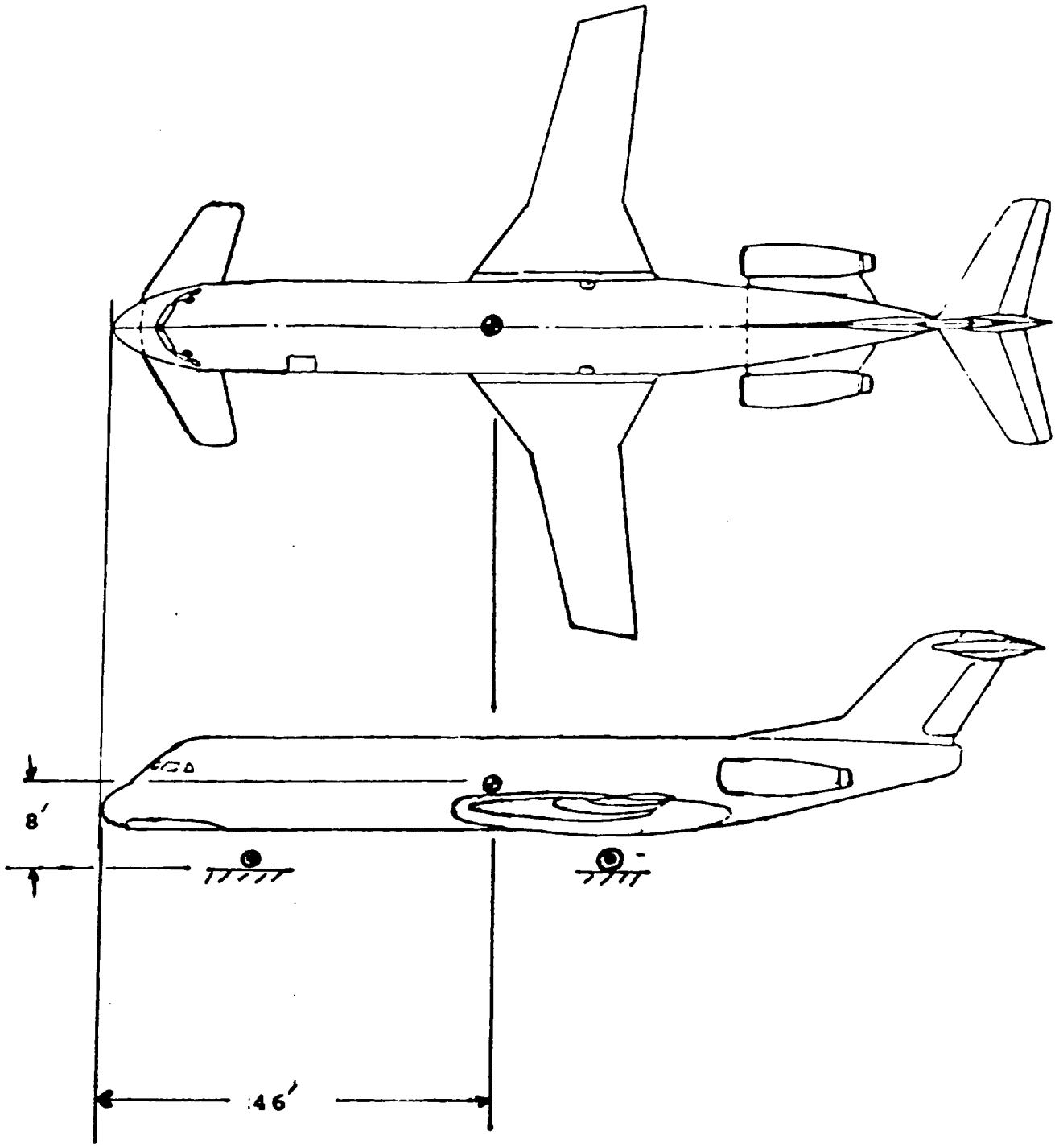

Figure 12: Center of Gravity Location

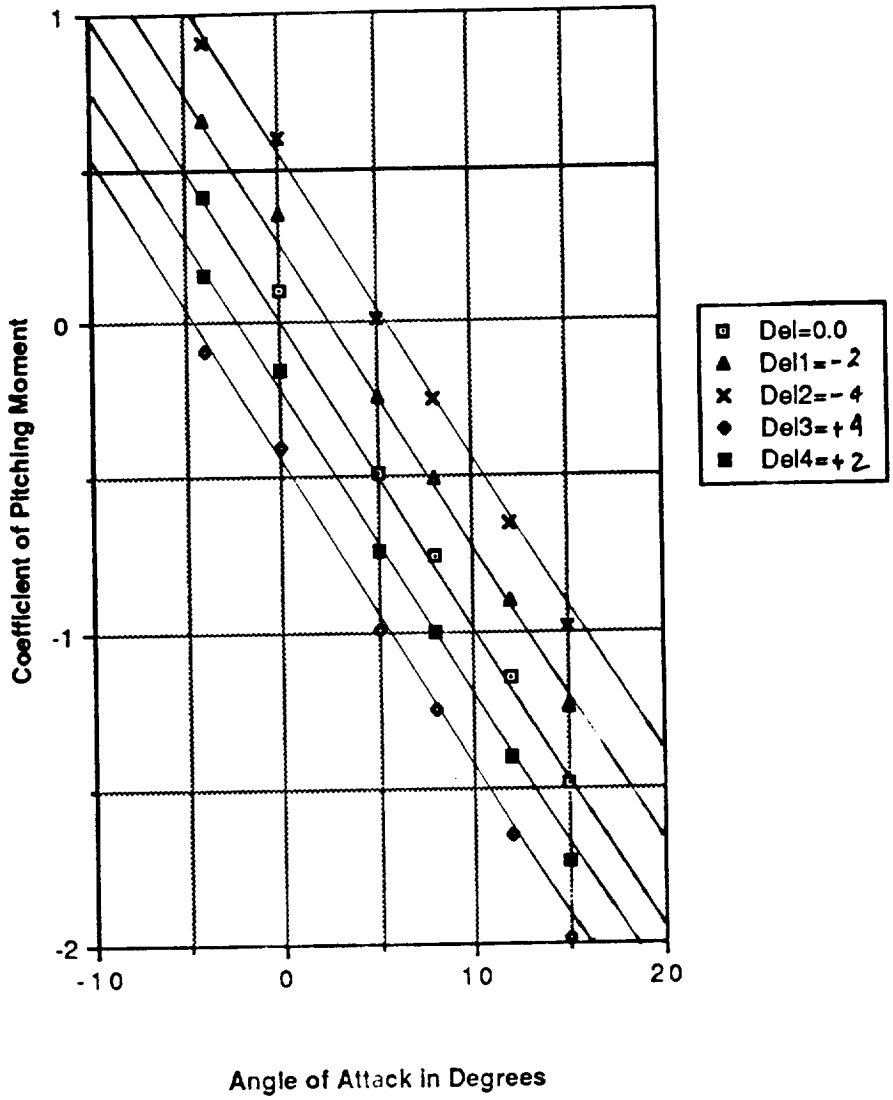

Figure 13: Pitching Moment Versus Angle of Attack for Tail Deflection

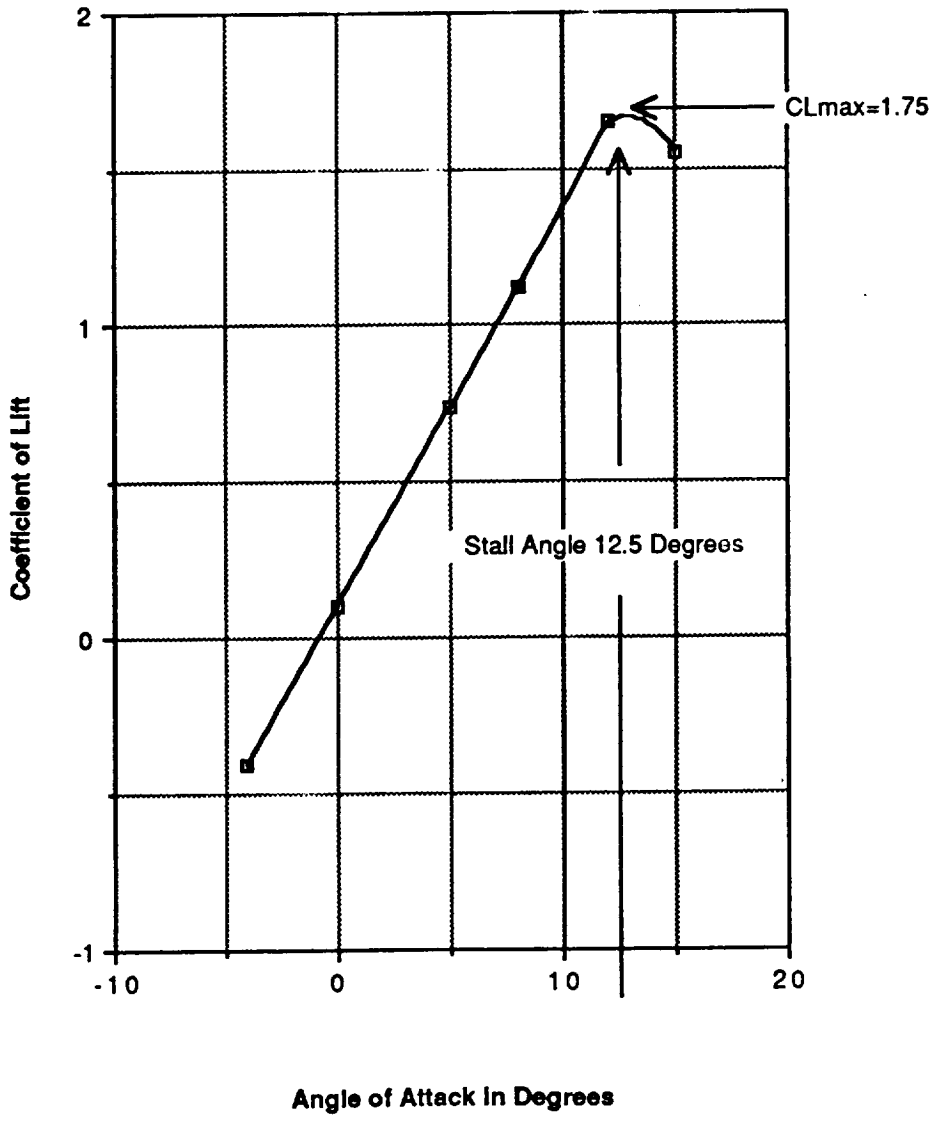

Figure 14: Lift Versus Angle of Attack

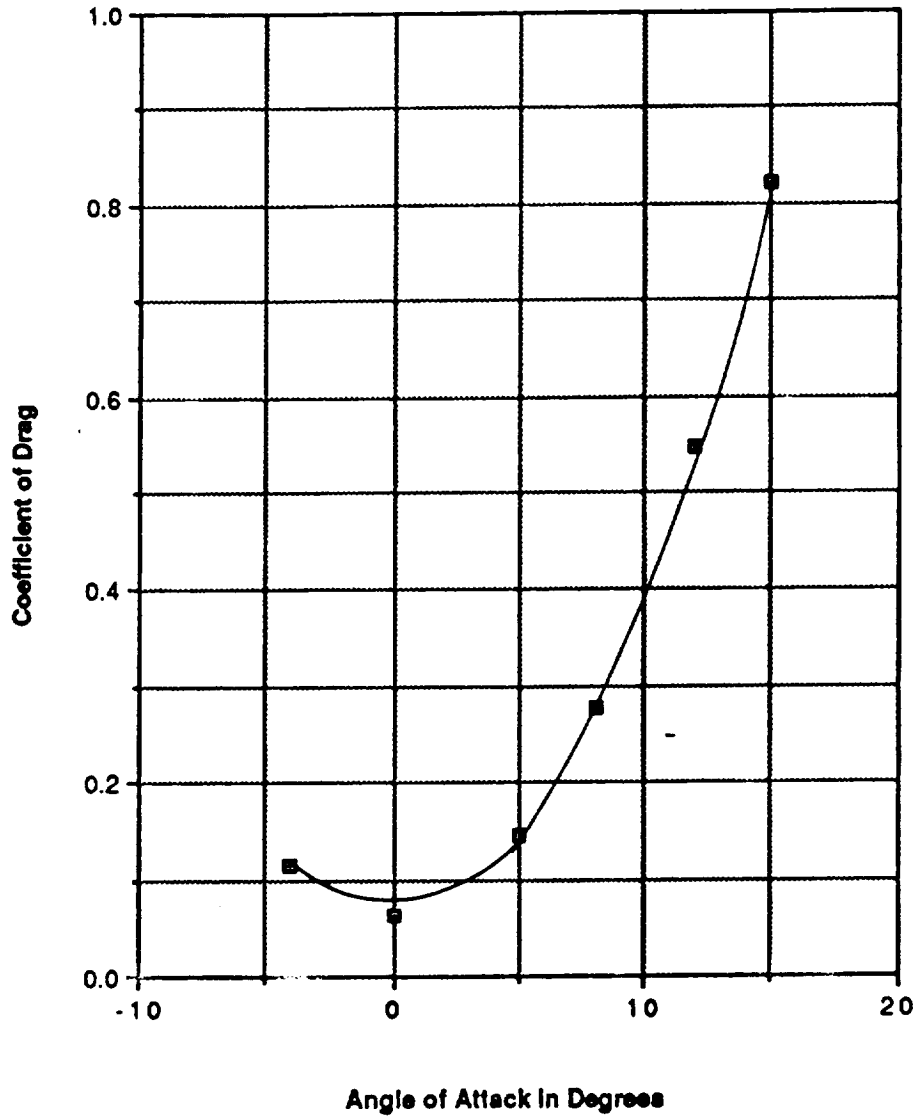

Figure 15: Drag Versus Angle of Attack

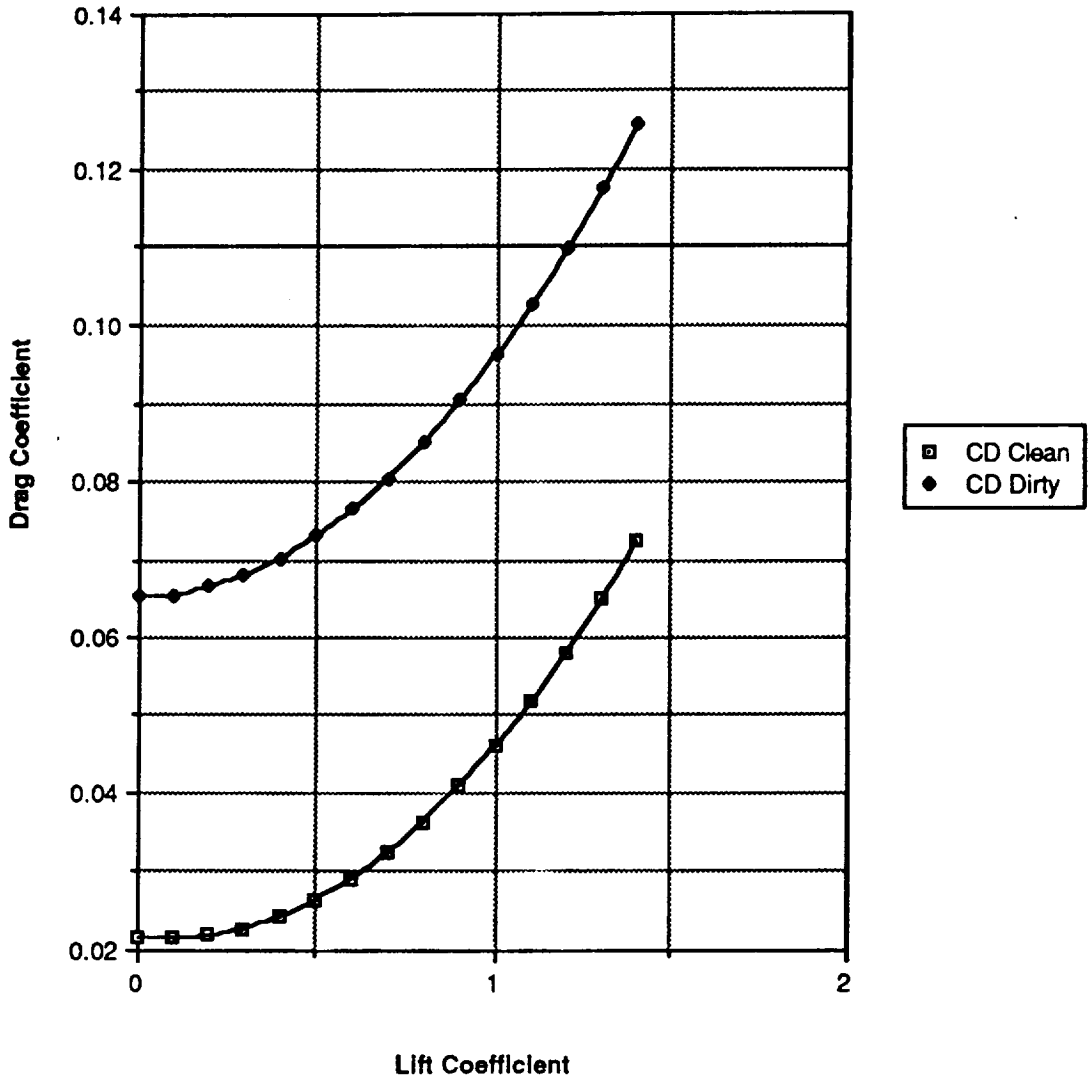

Figure 16: Basic Drag Polar

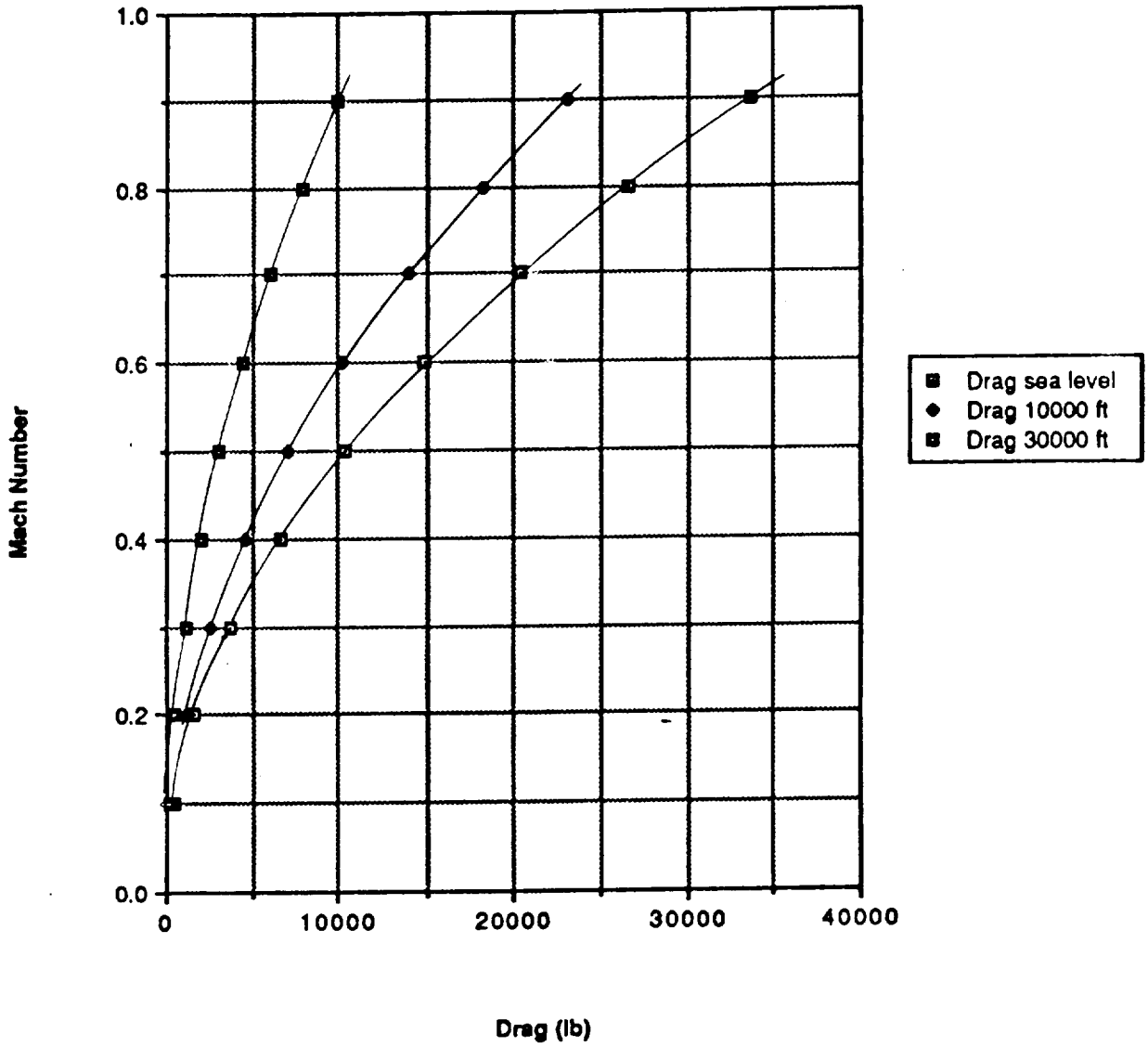

Figure 17: Mach Number Versus Drag

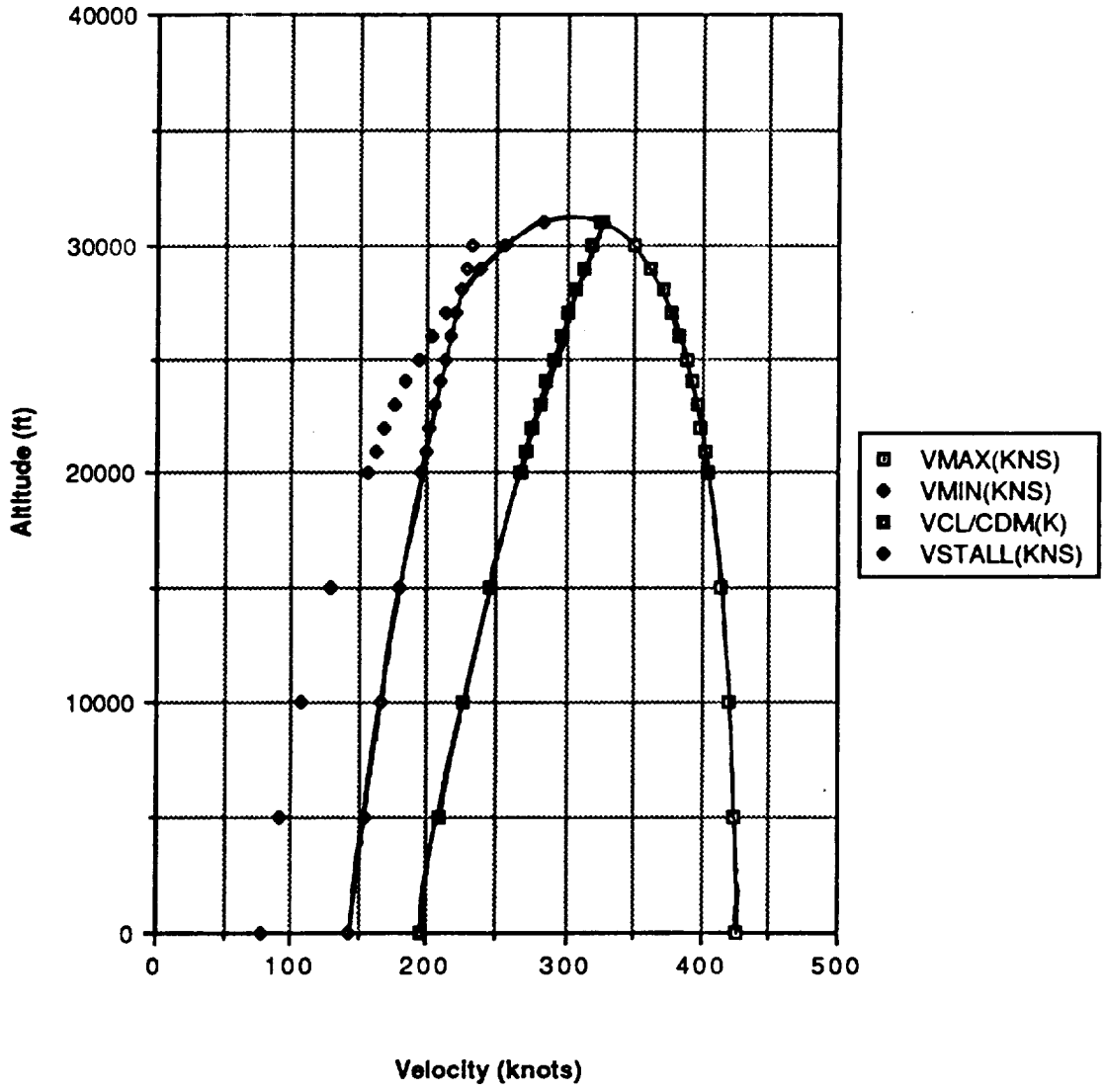

Figure 18: Altitude Versus Velocity

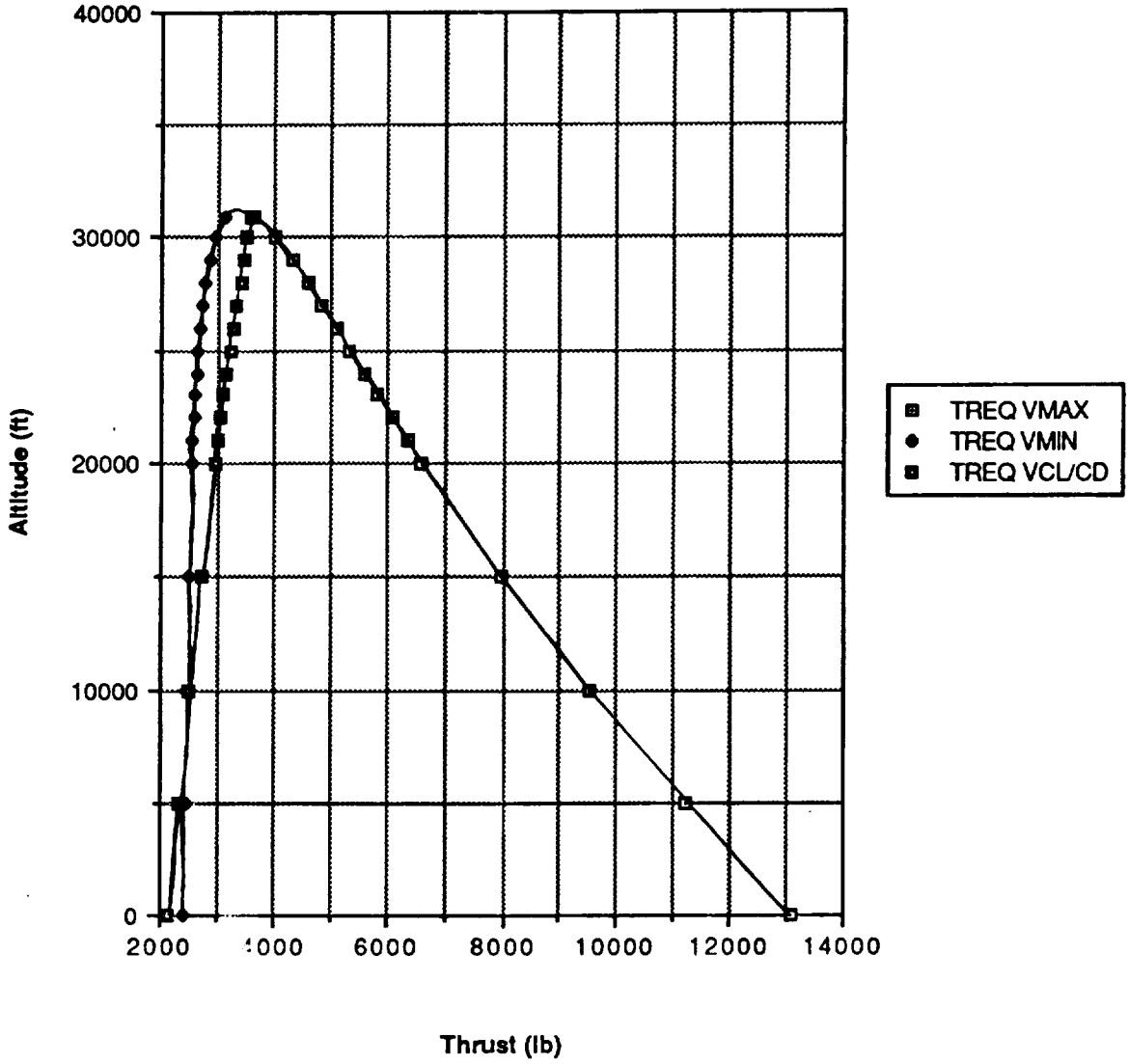

Figure 19: Altitude Versus Thrust Required

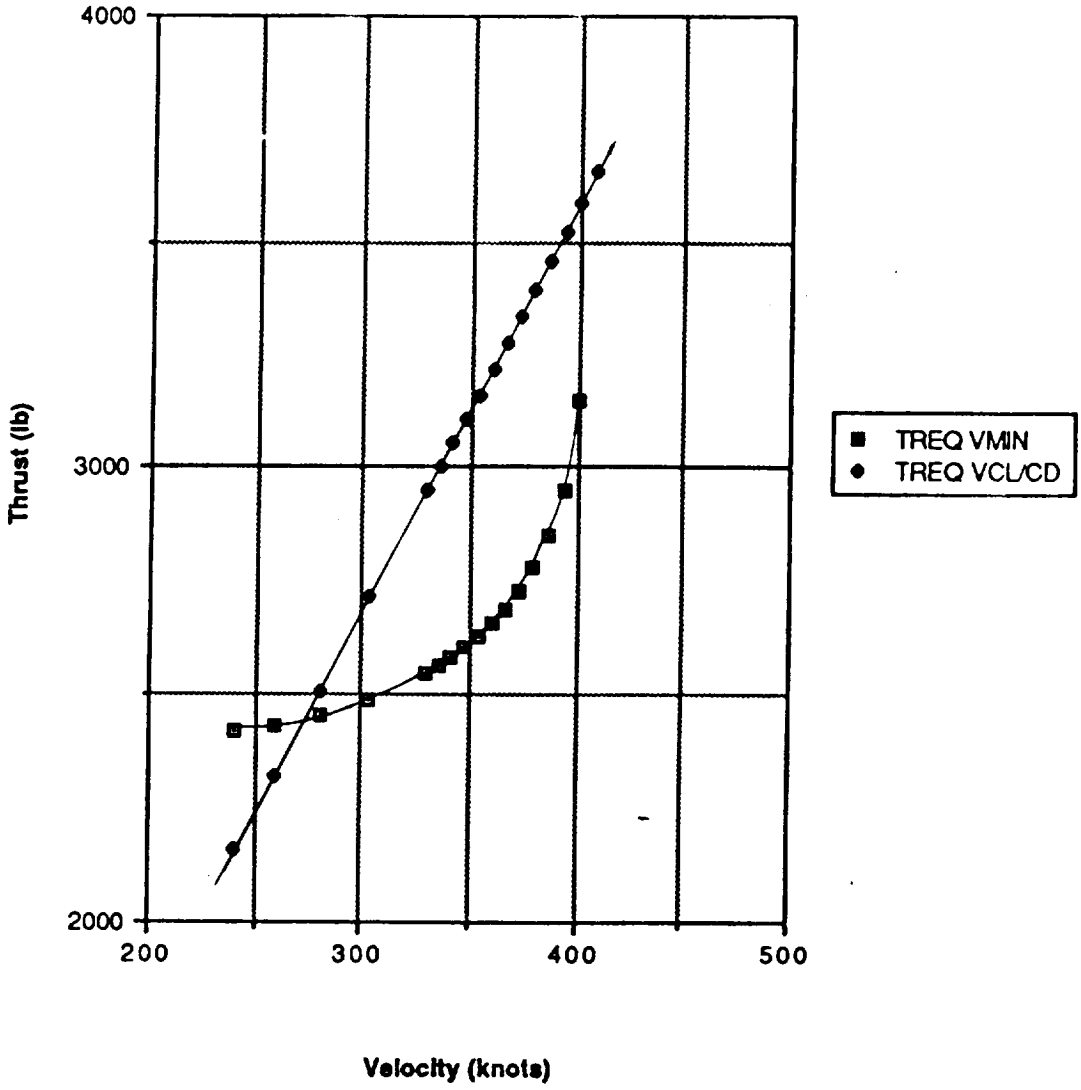

Figure 20: Minimum Thrust Required and Flight Thrust Versus Velocity at 30,000 Feet

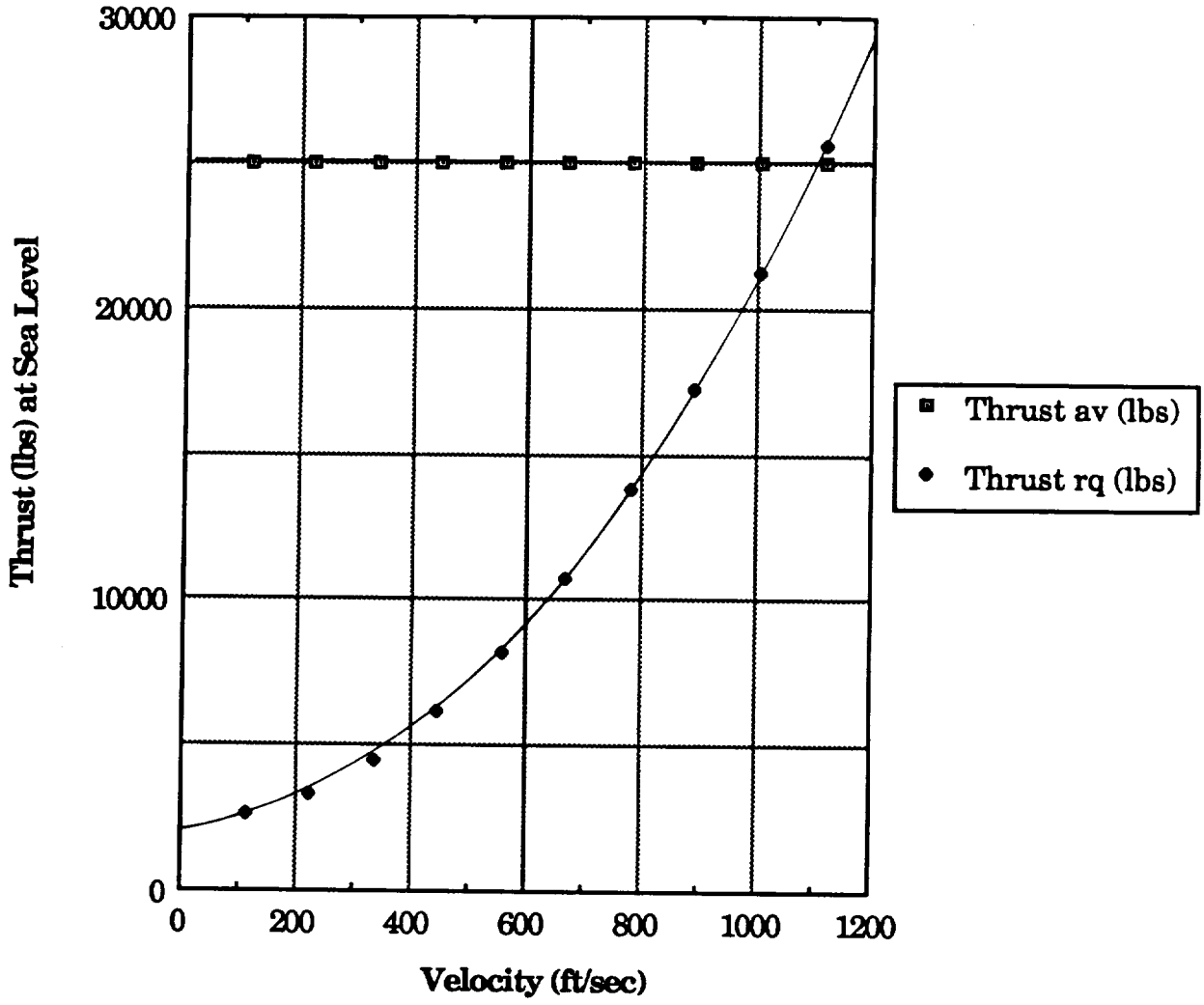

Figure 21: Thrust versus Velocity at Sea Level

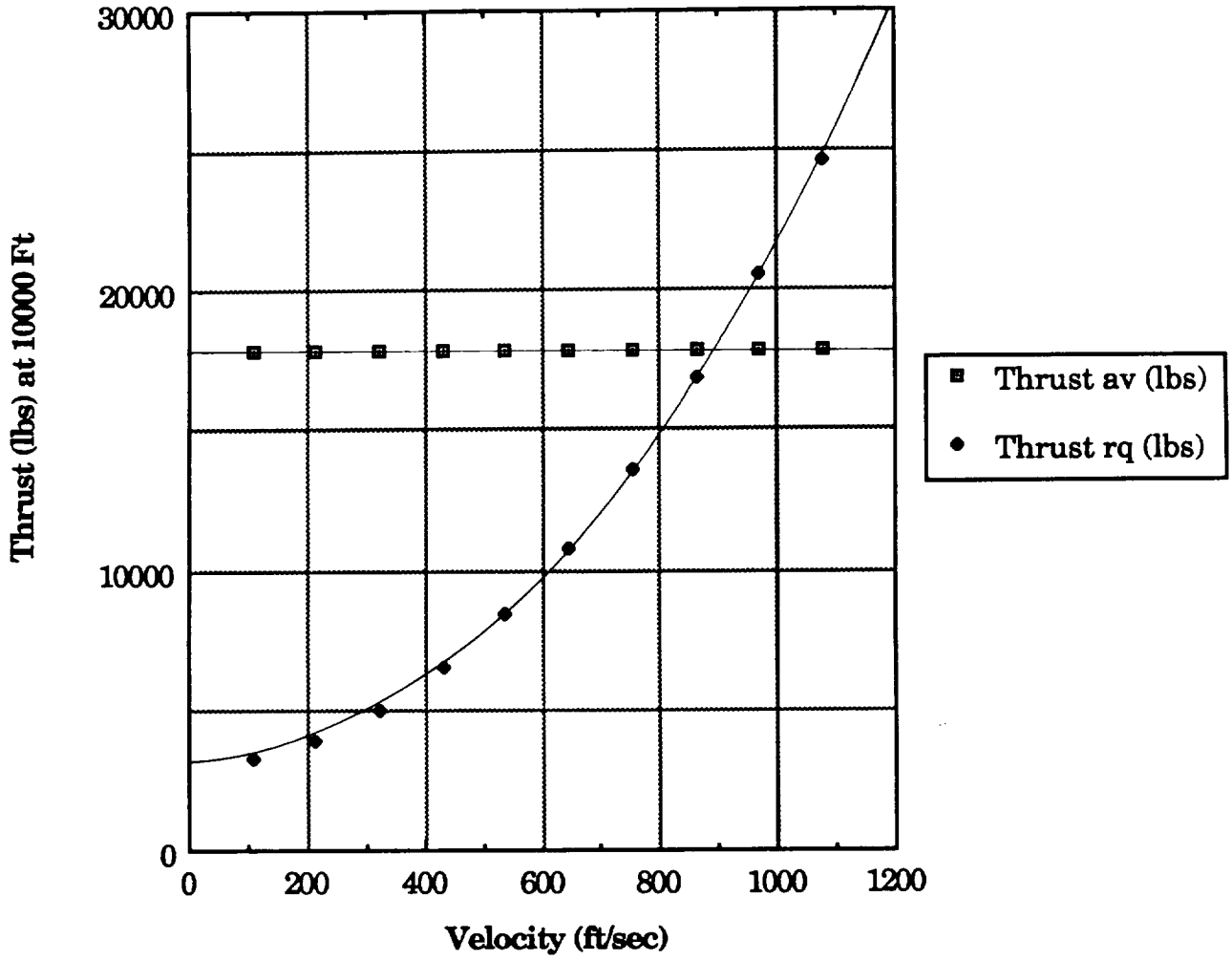

Figure 22: Thrust (lbs) versus Velocity at 10000 feet

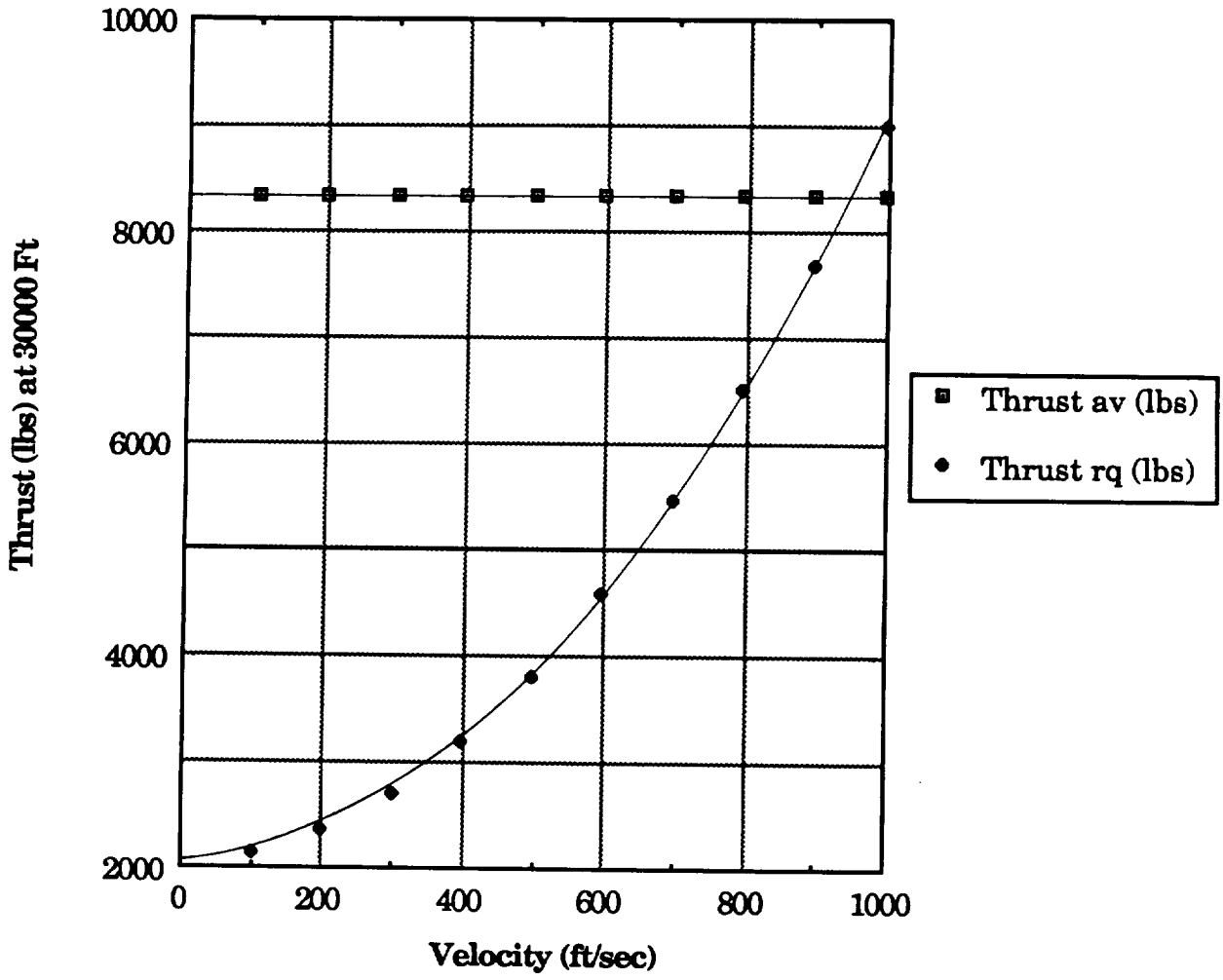

Figure 23: Thrust (lbs) versus Velocity at 30000

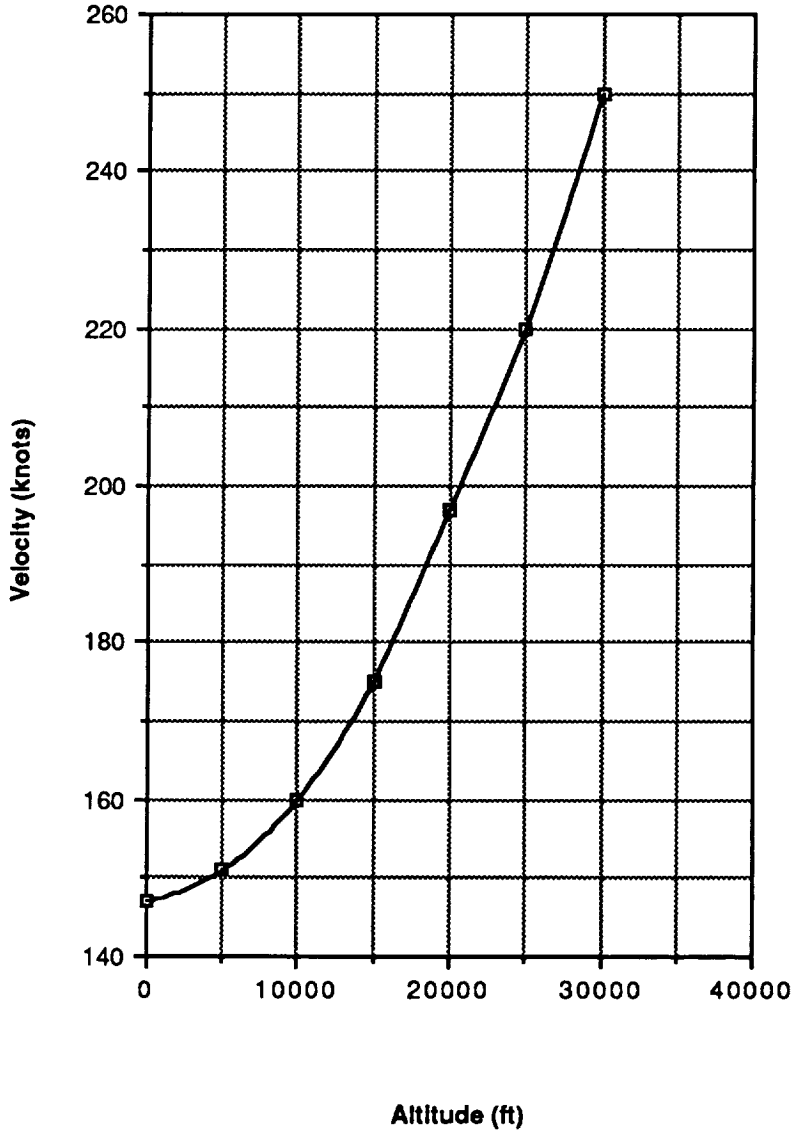

Figure 24: Stall Velocity Versus Altitude

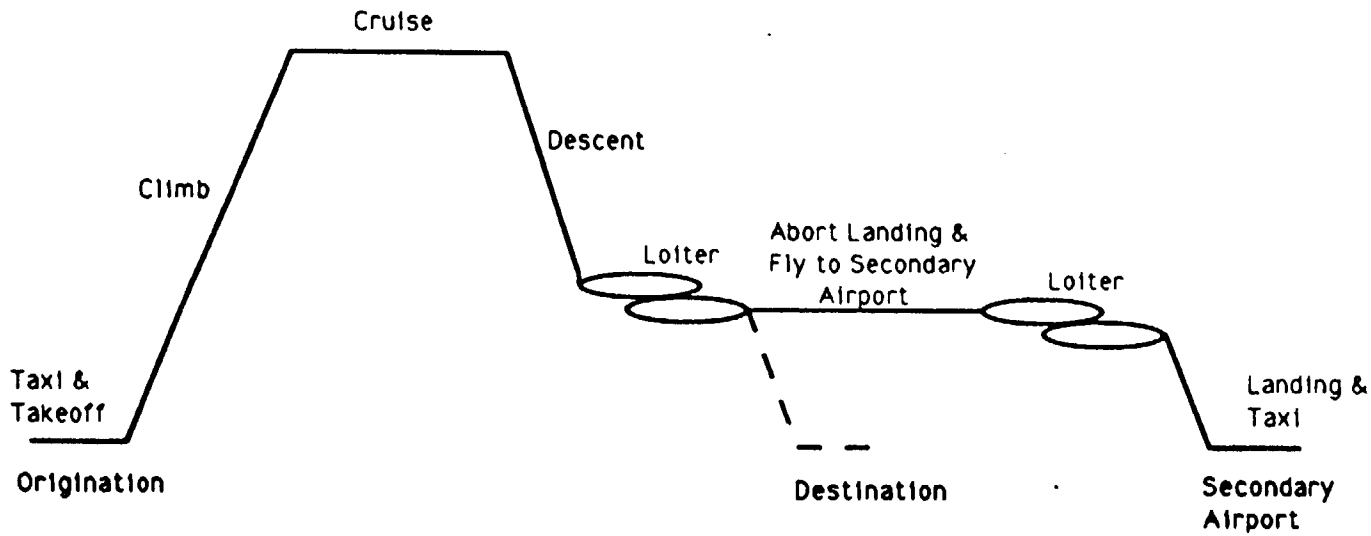

Figure 25: Mission Profile

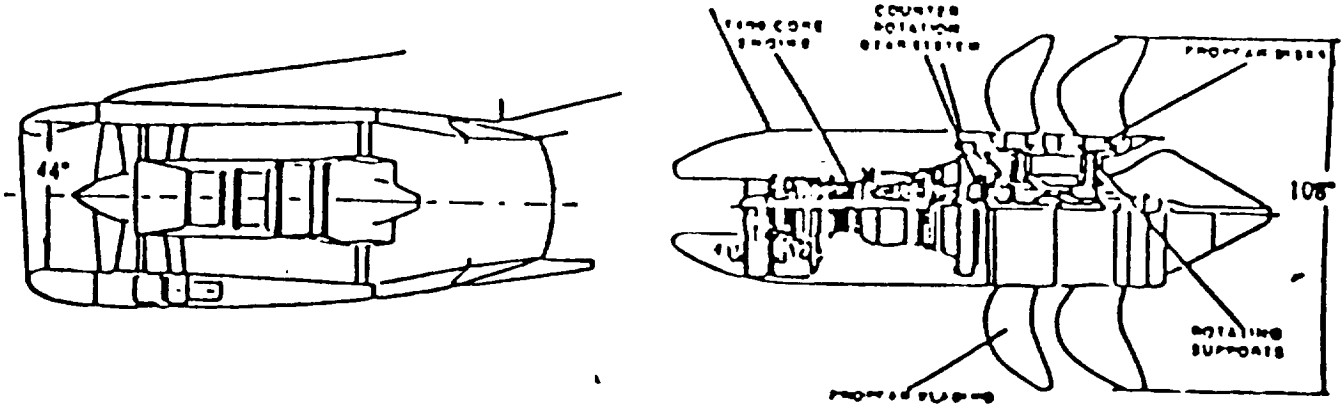

Installed T.O. thrust M = 0.2, ISA, SL	9200 lbf	+ 38 %	12700 lbf
Cruise thrust M = 0.75, 35 K	2420 lbf		2450 lbf
Cruise SFC	0.64 lb/lbf/h	- 20 %	0.51 lb/lbf/h
Propulsion weight incl. nacelle	3630 lb	+ 20 %	4350 lb
incl. pylon	4020 lb	+ 38 %	5560 lb

Figure 26: Comparisons of Engines

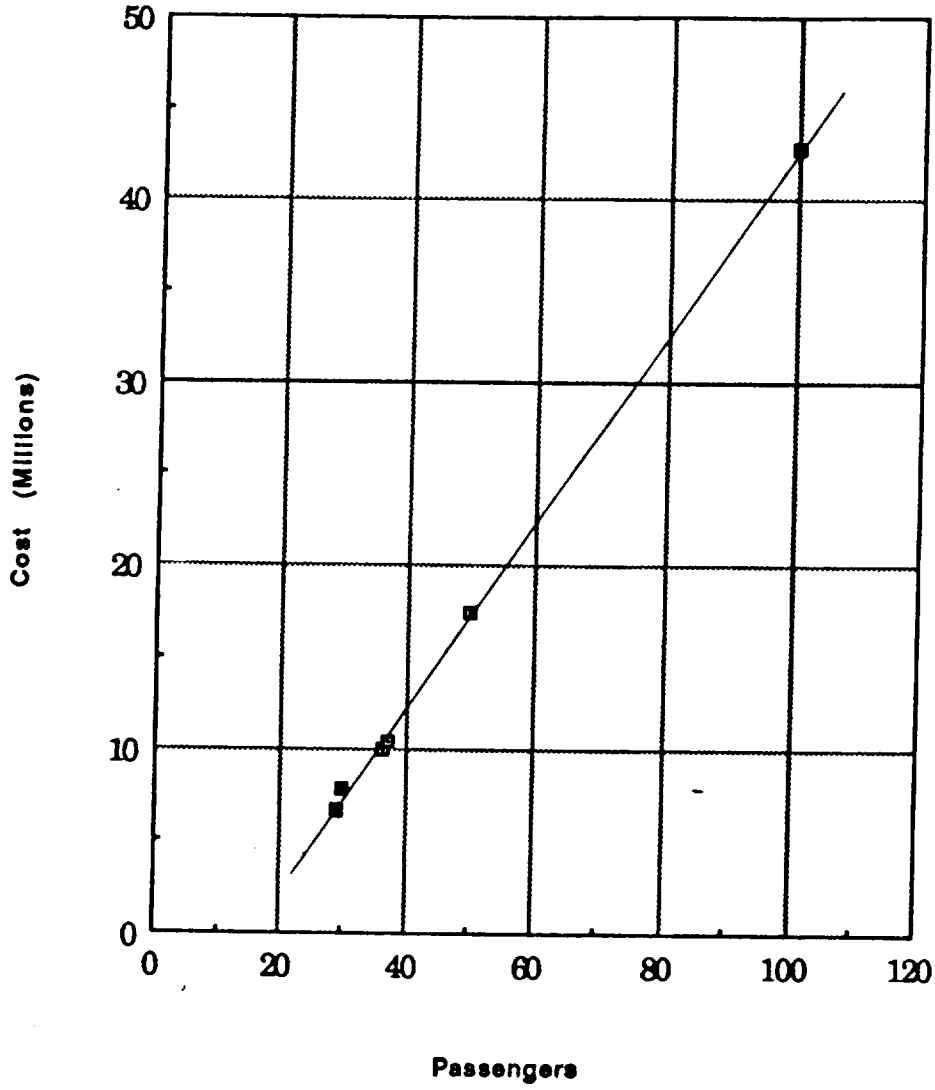

Figure 27: Developing Cost Versus Number of Passengers

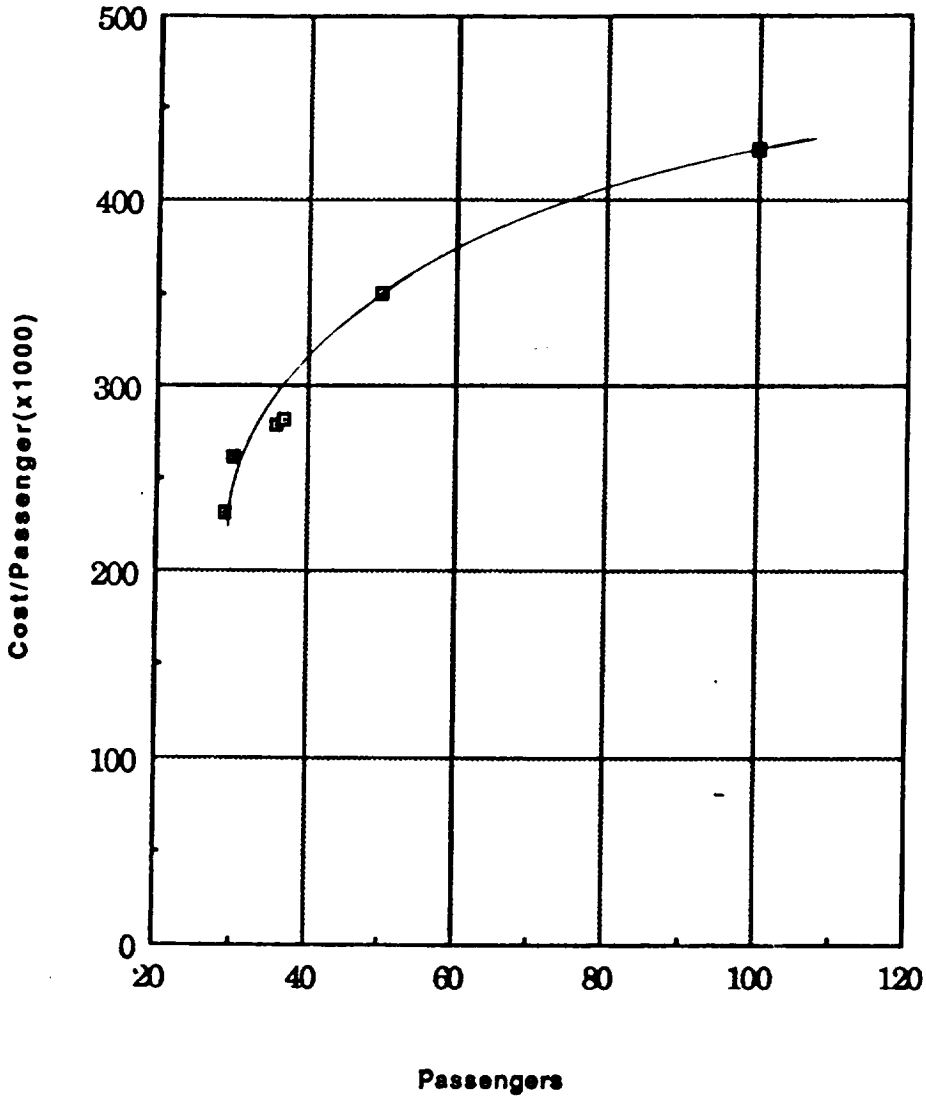

Figure 28: Per Passenger Cost Versus Number of Passengers

Table 1: Weight Calculations

Group	Weight (lb)
Passengers	13825
Fuel	22100
W fuse.	13323.769
W tail	1053.89426
w canard	658.683911
W wing	4590.24981
W ng	540.93768
W mg	1623.80935
W sc	1425.94975
W eng.	4500
W eng acc.	1636.36515
W avionics	2000
W fuel sys	1077.16093
W fltdeck seats	109.98
W pass seats	2402.25
W ac	1952.02616
W misc.	3975.49555
W baggage	3750
W nacelle	1300
W eng controls	336.365151
W pass service	225.078749
W instrum.	57.68
W elect.	2053.32047
W res fuel	1625
MZFW	63000
MTOW	80000
W empty	40870.5716
MTRW	80545.5716

Table 2: Center of Gravity Calculations

Component	CG location	xbar*weight	C.G. (ft)
fuselage	38	506303.223	
wing	55	252463.739	
tail	94	99066.0603	
canard	8	5269.47129	
engines	75	337500	
main gear	53	86061.8958	
nose gear	15	8114.0652	
avionics	15	30000	
fuel	45	1042972.24	
passengers	43	594475	
furnishings	40	337590.068	
baggage	35	131250	
eng acc	72	117818.291	
surface contro	53	75575.3368	
reserve fuel	40	65000	
Total no pass, full fuel		2898734.39	46.0331599
Total reserve fuel, pass		2646487.15	44.0563005
Total no pass, res fuel		1920762.15	45.1991132
Total full fuel, pass		3624459.39	44.9988661

Table 3: Drag Polar Data

Wing	Body	Canard
Re=4.0E+7	Re=4.70E+7	Re=3.0E+7
Cf=0.0023	Cf=0.002	Cf=0.002
Rls=1.08	Rwb=1.03	Rls=1.08
Swet=1200 ft^2	Swet=2600 ft^2	Swet=62.2^2
Sref=725 ft^2	Lref=95 ft^2	Sref=140^2

Tail	Vertical
Re3.0E+7	Re=3.0E+7
Cf=0.002	Cf=0.002
Swet=200 ft^2	Swet=215 ft^2
Sref=140 ft^2	Sref=255 ft^2

BIBLIOGRAPHY

1. Beer, Ferdinand P., and E. Russell Johnson, Jr. Vector Mechanics for Engineers. McGraw-Hill Company, New York, 1984.

2. Muvdi, B.B., and J.W. McNabb. Engineering Mechanics of Materials. Macmillian Publishing Company, New York, 1984.

3. Layton, Donald. Aircraft Performance. Matrix Publishers, Inc., Chesterland, Ohio, 1988.

4. Nicolai, Leland. Fundamentals of Aircraft Design. University of Dayton, Dayton, Ohio, 1975.

5. Piedmont Airlines Maintenance Training Department, Troubleshooting Index.

6. Pulaski, Mike, Chief Operation engineer. Packet of Aircraft Characteristics, Flight Handbook, USAir, Pittsburgh, Pennsylvania.

7. Raymer, Daniel P., Aircraft Design: A Conceptual Approach, AIAA Education Series, 1991.

8. Roskam, Jan. Methods for Estimating Drag Polars of Subsonic Airplanes.

9. Shevell, Richard, Fundamentals of Flight, Prentice Hall, Englewood Cliffs, New Jersey, 1989.

10. Taylor, John W. R., Jane's All The World's Aircraft 1988-1989, Jane's Information Group Limited, London, 1988.

11. Torenbeek, E. Synthesis of Subsonic Airplane Design. Delft University Press, 1982.

12. USAir, Ground Operations Familiarization Booklet. US Air Customer ServiceTraining, August 1989.

13. USAir, Passenger Loading Bridges. USAir Customer Service Training, July 1990.

APPENDIX A
STABILITY DATA

INPUT TABLES

TMF	TXCG	TWEIGH		
0.7500	4.18008000	0.0000		
31.50000000	-3.22998166E-02		15.00000000	4.99499989

CONFIGURATION 1
STEVE ELLIOT CONFIGURATION
GEOMETERIC VARIABLES

		BODY	WING	TAIL
XL	BODY LENGTH	105.0000		
DREF	REFERENCE LENGTH	8.0000		
AREF	REFERENCE AREA	725.0000		
DREFFT	REFERENCE LENGTH-FT.	8.0000		
AREFFT	REFERENCE AREA FT**2	725.0000		
YIY	MOMENT OF INERTIA	**********		
DBOD	BOATTAIL DIA. (CAL.)	0.3333		
XLBOD	BOATTAIL LENGTH (CAL.)	1.1667		
DCYODR	RATIO (CYL. DIA/REF. DIA)	1.3750		
BO	EXPOSED SEMI-SPAN		31.5000	14.0000
CR	ROOT CHORD		15.0000	10.0000
CT	TIP CHORD		4.9950	3.0000
TR	TAPER RATIO		0.3330	0.3000
AR	ASPECT RATIO		6.3016	4.3077
SWLE	LEADING EDGE SWEEP ANGLE (DEG)		15.9256	19.0914
SWTE	TRAILING EDGE SWEEP ANGLE (DEG)		-1.8500	-8.7500
CBAR/CR	MEAN GEOMETERIC CHORD/CR		0.7221	0.7128
YBAR/BO	SPANWISE LOCATION OF CBAR		0.4166	0.4103
XM/CR	CHORDWISE LOCATION OF CBAR		0.2496	0.1988
CENT/CR	DIST. FROM L.E. CR TO CENTROID		0.6107	0.5552
RB	RADIUS OF BODY AT FIN		5.5000	1.5000
XFIN	DIST. FROM NOSE TO L.E. CR		44.0000	92.0000
XCENT	DIST. FROM NOSE TO CENTROID		53.1602	97.5519
A/AR	AREA RATIO (2 FINS/AREF)		0.8687	0.2510
HINGE	DIST. FROM NOSE TO HINGE		44.0000	92.0000

---------- FLIGHT CONDITIONS ----------

FMACH= 0.75 XCG= 45.980 WEIGHT=******* ALT=******* RE=******** Q= 0.0

---------- SLOPES ----------

	BODY	WING	TAIL	TOTAL
KWB		1.121	1.077	
KBW		0.202	0.125	
CLA		5.681	4.657	
CP		0.435	0.376	
CNA	0.049	6.527	0.642	7.218
XCP	-504.746	50.521	95.756	50.751
CMACG	3.394	-3.705	-3.994	-4.304
CMQ	8.028	-4.206	-49.698	-45.876
CLP		-59.292	-2.178	-61.470
CLD		10.275	0.000	
CHA		-2.254	-0.116	
CHD		-1.915	-0.085	
CND		4.829	1.251	
CMDCG		0.929	-7.787	
SIGMA	0.001			

ALPHA	-4.000	0.000	5.000	8.000	12.000	15.000	18.000

CN	-0.507	0.000	0.634	1.022	1.552	1.960	2.381
CNW	-0.456	0.000	0.570	0.911	1.367	1.709	2.051
CNT	-0.098	0.000	0.123	0.196	0.294	0.368	0.442
CNB	-0.005	0.000	0.007	0.015	0.030	0.047	0.072
CD0	0.021	0.021	0.021	0.021	0.021	0.020	0.020
CDB	0.022	0.021	0.022	0.023	0.026	0.032	0.041
CDBAS	0.041	0.041	0.041	0.041	0.041	0.041	0.041
CD	0.116	0.063	0.146	0.277	0.547	0.822	1.161
CMCG	0.308	0.000	-0.389	-0.651	-1.049	-1.387	-1.759
CMWCG	0.259	0.000	-0.323	-0.517	-0.776	-0.970	-1.164
CMTCG	0.611	0.000	-0.763	-1.222	-1.832	-2.290	-2.749
CMBCG	-0.235	0.000	0.294	0.467	0.693	0.858	1.016
XCP	50.842	0.000	50.889	51.074	51.387	51.639	51.890
XCPW	50.521	50.521	50.521	50.521	50.521	50.521	50.521
XCPT	95.756	95.756	95.756	95.756	95.756	95.756	95.756
XCPB	-317.680	-504.746	-285.565	-210.260	-138.227	-101.584	-67.187
MARGN	4.771	4.771	4.771	4.771	4.771	4.771	4.771
CHW	0.158	0.000	-0.197	-0.318	-0.482	-0.610	-0.741
CHT	0.018	0.000	-0.022	-0.036	-0.055	-0.070	-0.086
CNTV	0.052	0.000	-0.065	-0.100	-0.139	-0.163	-0.183
FTRAT	0.466	0.000	0.471	0.492	0.527	0.557	0.586

ALPTRM	CNTRM	XCP	CMCG	HMW	HMT	GLOAD	ITER
0.00	0.000	0.000	0.000	0.000	0.000	0.000	0

INPUT TABLES

TMF	TXCG	TWEIGH		
0.7500	4.18008	0000.0000		
7.00000000	-0.57735026		6.00000000	2.51999998

CONFIGURATION 1
STEVE ELLIOT CONFIGURATION

GEOMETERIC VARIABLES		BODY	WING	TAIL
XL	BODY LENGTH	105.0000		
DREF	REFERENCE LENGTH	8.0000		
AREF	REFERENCE AREA	725.0000		
DREFFT	REFERENCE LENGTH-FT.	8.0000		
AREFFT	REFERENCE AREA FT**2	725.0000		
YIY	MOMENT OF INERTIA	**********		
DBOD	BOATTAIL DIA. (CAL.)	0.3333		
XLBOD	BOATTAIL LENGTH (CAL.)	1.1667		
DCYODR	RATIO (CYL. DIA/REF. DIA)	1.3750		
BO	EXPOSED SEMI-SPAN		7.0000	14.0000
CR	ROOT CHORD		6.0000	10.0000
CT	TIP CHORD		2.5200	3.0000
TR	TAPER RATIO		0.4200	0.3000
AR	ASPECT RATIO		3.2864	4.3077
SWLE	LEADING EDGE SWEEP ANGLE (DEG)		-4.5861	19.0914
SWTE	TRAILING EDGE SWEEP ANGLE (DEG)		-30.0000	-8.7500
CBAR/CR	MEAN GEOMETERIC CHORD/CR		0.7495	0.7128
YBAR/BO	SPANWISE LOCATION OF CBAR		0.4319	0.4103
XM/CR	CHORDWISE LOCATION OF CBAR		-0.0404	0.1988
CENT/CR	DIST. FROM L.E. CR TO CENTROID		0.3343	0.5552
RB	RADIUS OF BODY AT FIN		5.5000	1.5000
XFIN	DIST. FROM NOSE TO L.E. CR		2.0000	92.0000
XCENT	DIST. FROM NOSE TO CENTROID		4.0059	97.5519
A/AR	AREA RATIO (2 FINS/AREF)		0.0823	0.2510
HINGE	DIST. FROM NOSE TO HINGE		3.5000	92.0000

---------- FLIGHT CONDITIONS ----------

FMACH= 0.75 XCG= 45.980 WEIGHT=******* ALT=******* RE=******** Q= 0.

---------- SLOPES ----------

	BODY	WING	TAIL	TOTAL
KWB		1.390	1.077	
KBW		0.685	0.125	
CLA		4.009	4.657	
CP		0.130	0.376	
CNA	0.049	0.684	0.997	1.730
XCP	-504.746	2.781	95.756	41.866
CMACG	3.394	3.696	-6.200	0.890
CMQ	8.028	-39.914	-77.159	-109.045
CLP		-1.025	-2.178	-3.203
CLD		0.462	0.000	
CHA		0.021	-0.200	
CHD		0.014	-0.168	
CND		0.183	1.251	
CMDCG		4.193	-7.787	

SIGMA 0.001

ALPHA	-4.000	0.000	5.000	8.000	12.000	15.000	18.000

CN	-0.135	0.000	0.172	0.287	0.450	0.577	0.714
CNW	-0.048	0.000	0.060	0.096	0.143	0.179	0.215
CNT	-0.098	0.000	0.123	0.196	0.294	0.368	0.442
CNB	-0.005	0.000	0.007	0.015	0.030	0.047	0.072
CD0	0.021	0.021	0.021	0.021	0.021	0.020	0.020
CDB	0.022	0.021	0.022	0.023	0.026	0.032	0.041
CDBAS	0.041	0.041	0.041	0.041	0.041	0.041	0.041
CD	0.080	0.063	0.090	0.133	0.223	0.316	0.432
CMCG	0.015	0.000	-0.037	-0.120	-0.255	-0.363	-0.479
CMWCG	-0.258	0.000	0.323	0.516	0.774	0.968	1.161
CMTCG	0.611	0.000	-0.763	-1.222	-1.832	-2.290	-2.749
CMBCG	-0.235	0.000	0.294	0.467	0.693	0.858	1.016
XCP	46.871	0.000	47.681	49.329	50.506	51.008	51.349
XCPW	2.781	2.781	2.781	2.781	2.781	2.781	2.781
XCPT	95.756	95.756	95.756	95.756	95.756	95.756	95.756
XCPB	-317.680	-504.746	-285.565	-210.260	-138.227	-101.584	-67.187
MARGN	-4.114	-4.114	-4.114	-4.114	-4.114	-4.114	-4.114
CHW	-0.001	0.000	0.002	0.003	0.004	0.006	0.007
CHT	0.020	0.000	-0.025	-0.041	-0.062	-0.079	-0.096
CNTV	0.016	0.000	-0.018	-0.019	-0.018	-0.016	-0.015
FTRAT	0.832	0.000	0.855	0.903	0.940	0.956	0.966

ALPTRM	CNTRM	XCP	CMCG	HMW	HMT	GLOAD	ITER
0.00	0.000	0.000	0.000	0.000	0.000	0.000	0

APPENDIX B
PERFORMANCE DATA

thrust sea level

25000	mach	Velocity sea	kcl^2	Drag
	0.1	111.64	0.22488499	2640.03576
	0.2	223.28	0.05622125	3336.14305
	0.3	334.92	0.02498722	4496.32185
	0.4	446.56	0.01405531	6120.57218
	0.5	558.2	0.0089954	8208.89404
	0.6	669.84	0.00624681	10761.2874
	0.7	781.48	0.00458949	13777.7523
	0.8	893.12	0.00351383	17258.2887
	0.9	1004.76	0.00277636	21202.8967
	1	1116.4	0.00224885	25611.5762

thrust 10000 feet

17816.3	mach	Velocity10000	kcl^2	Drag
	0.1	107.74	0.30482679	3256.03616
	0.2	215.48	0.0762067	3904.35773
	0.3	323.22	0.03386964	4984.89366
	0.4	430.96	0.01905167	6497.64397
	0.5	538.7	0.01219307	8442.60866
	0.6	646.44	0.00846741	10819.7877
	0.7	754.18	0.00622095	13629.1811
	0.8	861.92	0.00476292	16870.789
	0.9	969.66	0.00376329	20544.6111
	1	1077.4	0.00304827	24650.6477

thrust 30000 feet

8333.6562	mach	Velocity30000	kcl^2	Drag
	0.1	99.485	0.65252748	2152.78348
	0.2	198.87	0.16329597	2360.08911
	0.3	298.455	0.07250305	2706.34019
	0.4	397.94	0.04078297	3190.70232
	0.5	497.425	0.0261011	3813.45363
	0.6	596.91	0.01812576	4574.59411
	0.7	696.395	0.01331689	5474.12378
	0.8	795.88	0.01019574	6512.04262
	0.9	895.365	0.00805589	7688.35064
	1	994.85	0.00652527	9003.04784

Height	Density	R/Rsealevel	th=th*r/rsea	th/2rsecds=tε	Tav.^2
0	2.38E-03	1.00E+00	1.00E+04	318.25	101,285.24
5000	2.05E-03	8.62E-01	8.62E+03	274.20	75,187.86
10000	1.76E-03	7.39E-01	7.39E+03	235.11	55,276.03
15000	1.50E-03	6.29E-01	6.29E+03	200.32	40,129.81
20000	1.27E-03	5.33E-01	5.33E+03	169.64	28,776.70
21000	1.22E-03	5.15E-01	5.15E+03	164.00	26,896.09
22000	1.18E-03	4.98E-01	4.98E+03	158.47	25,112.95
23000	1.14E-03	4.81E-01	4.81E+03	153.10	23,440.14
24000	1.10E-03	4.65E-01	4.65E+03	147.85	21,860.59
25000	1.07E-03	4.49E-01	4.49E+03	142.77	20,381.99
26000	1.03E-03	4.33E-01	4.33E+03	137.80	18,988.36
27000	9.93E-04	4.18E-01	4.18E+03	132.97	17,680.01
28000	9.58E-04	4.03E-01	4.03E+03	128.27	16,452.35
29000	9.24E-04	3.89E-01	3.89E+03	123.70	15,300.64
30000	8.91E-04	3.75E-01	3.75E+03	119.25	14,221.04
31000	8.58E-04	3.61E-01	3.61E+03	114.93	13,209.23
32000	8.27E-04	3.48E-01	3.48E+03	110.73	12,261.42
33000	7.97E-04	3.35E-01	3.35E+03	106.65	11,374.30
34000	7.67E-04	3.23E-01	3.23E+03	102.69	10,544.68
35000	7.38E-04	3.11E-01	3.11E+03	98.84	9,768.68

t2-kw2/cds	(t-kw2/cds2)	Tav.+()^.5	Tav.-()^.5	Vmax	Vmin
88,336.50	297.21	615.47	21.039	719.62	133.05
62,239.11	249.48	523.68	24.726	715.13	155.39
42,327.28	205.74	440.84	29.373	708.59	182.90
27,181.07	164.87	365.19	35.457	698.68	217.71
15,827.96	125.81	295.45	43.828	682.91	263.03
13,947.34	118.10	282.10	45.901	678.68	273.76
12,164.21	110.29	268.76	48.179	673.90	285.33
10,491.39	102.43	255.53	50.674	668.52	297.71
8,911.85	94.40	242.26	53.451	662.38	311.13
7,433.25	86.22	228.98	56.549	655.35	325.68
6,039.61	77.71	215.51	60.083	647.15	341.70
4,731.27	68.78	201.75	64.182	637.42	359.52
3,503.60	59.19	187.46	69.075	625.58	379.74
2,351.89	48.50	172.19	75.199	610.54	403.48
1,272.29	35.67	154.92	83.583	589.81	433.22
260.48	16.14	131.07	98.792	552.61	479.76
-687.32	#NUM!	#NUM!	#NUM!	#NUM!	#NUM!
-1,574.44	#NUM!	#NUM!	#NUM!	#NUM!	#NUM!
-2,404.07	#NUM!	#NUM!	#NUM!	#NUM!	#NUM!
-3,180.06	#NUM!	#NUM!	#NUM!	#NUM!	#NUM!

Vmax (Knots)	Vmin (Knots)	V for Cl/CDm	VCL/CDm (k)	Vstall	Vstall (knots)
425.81	78.73	329.12	194.74	240.888688	142.537685
423.15	91.95	354.57	209.80	259.517125	153.560429
419.28	108.23	382.91	226.58	280.26492	165.83723
413.42	128.82	414.83	245.46	303.624052	179.659202
404.09	155.64	450.79	266.74	329.945864	195.234239
401.59	161.99	458.47	271.29	335.568108	198.561011
398.76	168.83	466.40	275.98	341.372489	201.995556
395.58	176.16	474.51	280.78	347.306501	205.506805
391.94	184.10	482.86	285.72	353.41702	209.122497
387.78	192.71	491.39	290.76	359.659298	212.816153
382.93	202.19	500.17	295.96	366.084303	216.617931
377.17	212.73	509.17	301.29	372.676767	220.518797
370.16	224.70	518.42	306.76	379.442502	224.522191
361.27	238.74	527.91	312.37	386.389721	228.632971
349.00	256.35	537.65	318.14	393.523024	232.85386
326.99	283.88	547.67	324.06	400.851592	237.190291
#NUM!	#NUM!	557.96	330.15	408.383079	241.646792
#NUM!	#NUM!	568.53	336.41	416.123028	246.226644
#NUM!	#NUM!	579.40	342.84	424.076922	250.93309
#NUM!	#NUM!	590.58	349.45	432.258932	255.774516

treq Vmax	treq Vmin	treq VCl/Cd
13083.9975	2419.07207	2155.8833
11202.677	2434.26704	2322.60236
9517.61423	2456.7247	2508.28905
7996.09658	2491.562	2717.34645
6618.36375	2549.09523	2952.91898
6358.78751	2564.99428	3003.23641
6101.12087	2583.18438	3055.18392
5847.38242	2603.96265	3108.29159
5595.04809	2628.10872	3162.97895
5345.19204	2656.2942	3218.84552
5094.59818	2689.98539	3276.34744
4842.04709	2731.04229	3335.34806
4584.16339	2782.72335	3395.89941
4314.54635	2851.25333	3458.07498
4018.27227	2951.49749	3521.91596
3628.46984	3150.15069	3587.5045
#NUM!	#NUM!	3654.90911
#NUM!	#NUM!	3724.17938
#NUM!	#NUM!	3795.36441
#NUM!	#NUM!	3868.59101